AD-A034 164 AUBURN UNIV ALA DEPT OF MECHANICAL ENGINEERING F/G 13/10
PERFORMANCE OF AIR-AUGMENTED WATERJET THRUSTERS.(U)
NOV 76 D F DYER, G MAPLES, H T CANSLER N00014-75-C-0936
UNCLASSIFIED NL

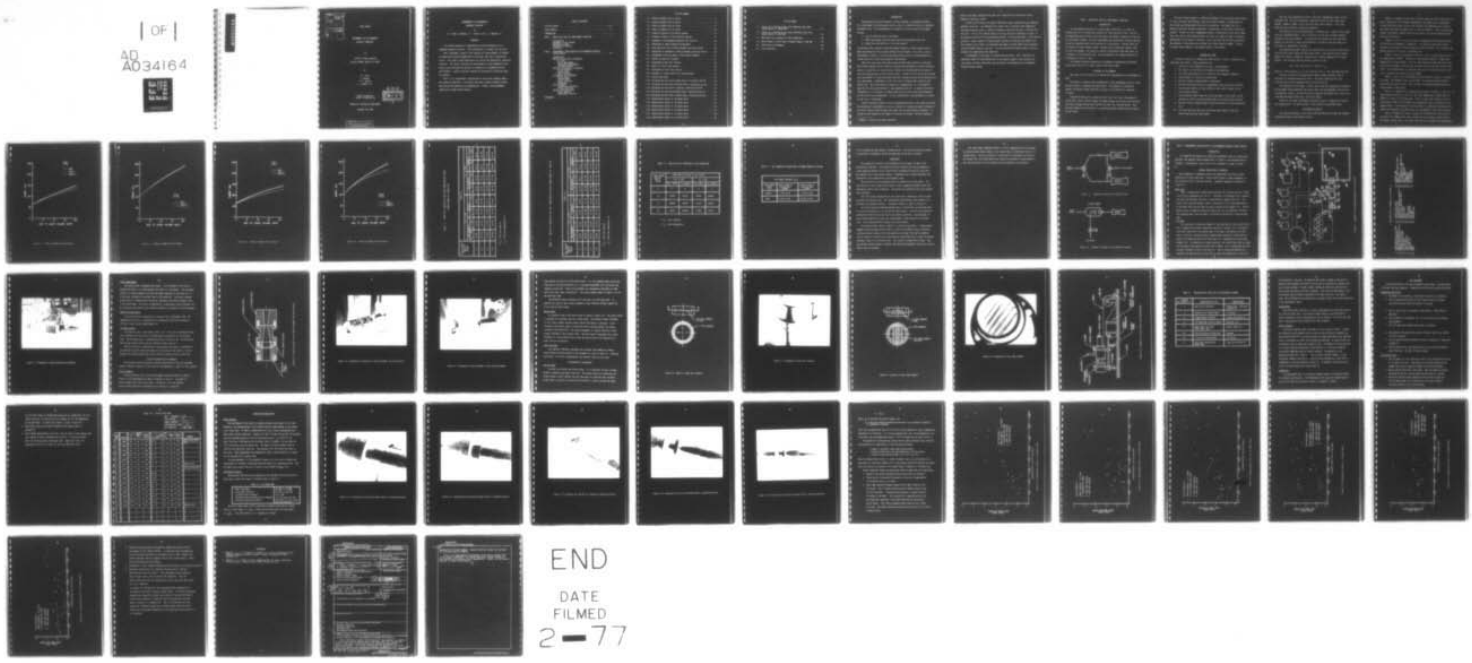

END

DATE
FILMED
2-77

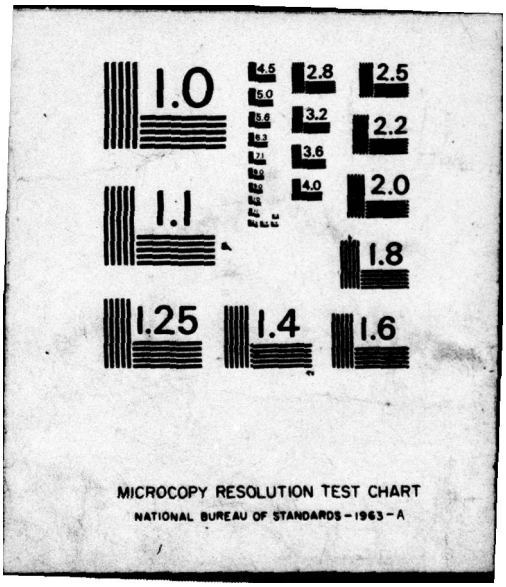
1.0
1.1
1.25
1.4
1.6
1.8
2.0
2.2
2.5
2.8
3.2
3.6
4.0
4.5
5.0
MICROCOPY RESOLUTION TEST CHART
NATIONAL BUREAU OF STANDARDS - 1963 - A

FINAL REPORT

PERFORMANCE OF AIR-AUGMENTED WATERJET THRUSTERS

for

Office of Naval Research

Contract Number N00014-75-C-0936

by

D. F. Dyer
G. Maples
H. T. Cansler
J. C. Maxwell, Jr.

Auburn University
School of Engineering

Mechanical Engineering Department

November 30, 1976

PERFORMANCE OF AIR-AUGMENTED WATERJET THRUSTERS

by

D. F. Dyer, G. Maples, H. T. Cansler, and J. C. Maxwell, Jr.

ABSTRACT

This report describes an investigation of the performance of air-augmented waterjet thrusters. The investigation is divided into two parts.

Part 1 describes a study of the injection of large diameter air bubbles to reduce heat transfer between the air and water and, thus, increase the thrust. This study is done analytically by solving the appropriate, governing equations. The results indicate that the approach is very worthwhile since thrust can be increased ten percent as compared to air-augmentation with small bubbles. Several practical systems are discussed for injecting large air bubbles.

Part 2 is an experimental investigation of the thrust produced under a wide range of conditions. The results show that a thrust increase of more than 20% can be achieved by air-augmentation. Further, the performance improves for larger thrust nozzles.

TABLE OF CONTENTS

LIST OF FIGURES

LIST OF TABLES

INTRODUCTION

The pump-driven waterjet becomes a strong contender as a propulsion system for a high-speed, non-displacement vehicle, such as a Hydrofoil Craft or a Captured-Air-Bubble Craft. The disadvantages of a propeller driven system at high speeds include:

1. Loss in efficiency due to cavitation,
2. Wake interference with the screw from non-displacement ships, and
3. Weight and unreliability of the drive systems.

On the other hand, waterjet system performance inproves at higher speeds and the wake interference and drive system problems are eliminated. As a result, there is considerable interest in building high speed marine craft utilizing waterjet propulsion both for military and commercial applications.

About four years ago, the authors began research under contract to the Naval Ship Systems Command on their concept to improve the performance, (thrust and efficiency), of a waterjet, by injecting high pressure gas from the power plant used to drive the waterjet pump into the thrust nozzle. A report [1]* on this research shows that considerable (in some cases more than 20%) increase in thrust can be obtained with this improvement. Experiments in the first year of research were limited to one nozzle size. Due to the potential shown by gas augmentation, it is desirable to know the full-scale performance of a gas-augmented waterjet. To obtain this design information, it is necessary to study various nozzle sizes so that the performance of this device can be determined. In this investigation, the performance of nozzles of two sizes is determined.

Another important element in the gas-augmented waterjet is the injection process. An experimental investigation of various injectors is required in order to design an efficient injector which provides the proper size and distribution of bubbles. To accomplish this objective, two types of injectors are tested: one with injection

---

* Numbers in brackets designate references.

ports in the water stream and the other with injection ports around the circumference of the water stream.

In their earlier work, the authors identified a major problem with gas-augmented waterjet propulsion. The compressed air usually has a relatively high temperature and thermal energy, which is rapidly dissipated as heat once the gas is injected into the water. Part of this thermal energy in the gas would be transformed to thrust in the expansion process if the two-phase heat transfer is greatly decreased. In this work an analytical study is made into reducing heat transfer by increasing the bubble size. This object of this study is to determine the amount of thrust which can be captured from the thermal energy in the gas. It is also desired to examine several practical systems for accomplishing this objective.

The remainder of the report is divided into two parts: Part 1 describes the analytical study for transforming more of the thermal energy in the injection gas into thrust, and Part 2 describes the experimental investigation of air-augmented waterjet thrust nozzles.

PART 1. ANALYTICAL STUDY OF LARGE BUBBLE INJECTION

INTRODUCTION

The gas-augmented waterjet has recently been studied [1] as a means to increase thrust in a conventional waterjet for short periods of time. Previous gas-augmented waterjet studies considered small gas bubbles injected into the flow. In those models studied, the thrust improvement came essentially from work done by the gas in expanding from a high pressure to a low pressure. The gas itself has the capacity to store thermal energy. However, due to high heat transfer rates for small gas bubbles, this energy is quickly transferred to the water which is, in essence, an infinite heat sink. Thus, the potential for thermal energy to be transformed to thrust is lost.

This chapter explores analytically one method of transferring the thermal energy from a hot gas to a water stream in the form of work.

STATEMENT OF THE PROBLEM

The object of this section is to provide the requirements for the mathematical model.

The physical situation under consideration is the simultaneous flow of liquid and gas through a converging-diverging nozzle. The problem is to determine whether the thermal energy contained in the gas can be effectively converted to thrust.

Considering the gas as a system by itself, the first law of thermodynamics states that, given a specific amount of thermal energy, any process that maximizes the kinetic energy and work must minimize the heat loss from the system. Thus, the main concern of this analysis is to minimize the heat transferred from the gas to the liquid.

The rate of heat transfer is predicted by Newton's law of cooling, which states, all other variables held constant, that the net heat transfer is porportional to the surface area through which the heat is transferred. This means that for a spherical body that the heat transferred is porportional to the radius of the body squared. The mass of such a homogeneous system is porportional to the radius cubed. Thus, the ratio of heat transferred per unit mass of a spherical body is inversely porportional to the radius of the body. For a given mass the net heat transferred must decrease if the bodies are collected into larger spherical bodies. The use of larger radius bubbles is the method studied in this report.

MATHEMATICAL MODEL

In order to construct a mathematical model certain 'a priori' assumptions are made about the process. These assumptions are:

1. The flow is time independent and quasi one-dimensional.
2. The nozzle is frictionless and thermally non-conducting.
3. The liquid phase behaves as an isochloric and isothermal subsystem.
4. The gas phase is a chlorically perfect gas.
5. The mass transfer between phases is negligible.
6. The gas-liquid phase mixture is homogeneous at any given nozzle station.
7. The gas phase pressure at each station in the nozzle is equal to the local stream pressure.
8. The gas bubbles remain spherical during residence in the nozzle, do not coalese nor divide, and have uniform radii at any given nozzle station.
9. The heat transfer between phases follows the process of forced convection only.
10. The large radii gas phase has significant mass effects so that the bubbles move with the liquid phase.

The first nine assumptions as well as the basic computational model are due to Maxwell [2]. The last assumption is made specifically for the large radius bubbles. Maxwell's model is only valid for small radius bubbles. Thus, some modifications of the basic program are necessary.

The prediction of the drag coefficient in reference [2] is based on the assumption of an unbounded medium. This is obviously not the case as bubble diameter approaches the cavity diameter. To account for wall effects for the large radii bubbles, an arbitrarily large drag coefficient is chosen so that the velocity of each phase is approximately the same.

The computational model requires the specification of an initial velocity profile and local sonic velocity at the nozzle throat. The velocity profile used by Maxwell [2] results in numerical instabilities in making computations for large bubbles. The following modified velocity profile is used

$$V(x) = 200\ (\tanh\ (10\,x - 3) + \tanh\ 3) + V_o \quad .$$

where V is local velocity, V_o is inlet velocity, and x is the coordinate position.

The basic premise of the computational model assumes supersonic flow is achieved in a converging-diverging nozzle. The local properties and cross-sectional area are then computed from the velocity profile.

The limitation of this model is mostly due to the time independence assumption. As the bubble radius approaches the throat radius the time dependent terms may not be neglected. Hence, a restriction must be placed on the bubble size so that at no time does the bubble radius equal the nozzle radius.

Details of the model and computer program are given in reference [2] and are not repeated here. The modifications to that program are described above.

DISCUSSION OF RESULTS

The results described in this section were obtained by the model and computer program described in the previous section.

Figures 1.1 through 1.4 are plots of thrust versus the inlet volume ratio of gas to liquid with inlet pressure, temperature, and bubble radii as parameters. In each individual graph, the gas inlet pressure and temperature are fixed and two curves are shown for bubble radii of .025 and .00025 ft. Also, on each graph results for adiabatic bubble expansion are given to indicate the maximum thrust which can be achieved.

Figures 1.1 and 1.2 are for an inlet air temperature of 750°R and pressures of five and ten atmospheres, respectively. It should be noted that with the exception of the lower limit the curves are tightly grouped. This is because the thermal potential in the gas is relatively low.

Figures 1.3 and 1.4 correspond to Figures 1.1 and 1.2 except that the inlet air temperature is 1000°R. The effect of the thermal potential is shown more dramatically in these figures. Note the large disparity between the small radii curve and the adiabatic limit and the closeness of the large radii curve to this limit. This substantiates our assertion that more of the thermal energy in the gas is converted into thrust for large bubbles.

Tables 1.1 and 1.2 are the computed results from which Figures 1.1 through 1.4 are taken. The adiabatic cases are obtained by assigning the heat transfer coefficient the value of zero. Thus, no heat is exchanged between the gas and liquid phases in these cases.

Table 1.3 is important in interpreting the results in Tables 1.1 and 1.2. In those tables the thrust is less for a gas inlet temperature of 1000°R than for 750°R for a given inlet volume ratio. Table 1.3 shows that the mass of gas is significantly lower for the 1000°R inlet temperature, thus, accounting for the reduced thrust. The lower mass flow rate results in a decrease in energy for the 1000°R case compared to the 750°R case, and, consequently, less thrust increase.

Table 1.4 compares net thrust increase for equivalent mass flow ratios at different inlet bubble radii, thus, showing the net increase in thrust due to the thermal energy alone. This table shows that the increased inlet temperature

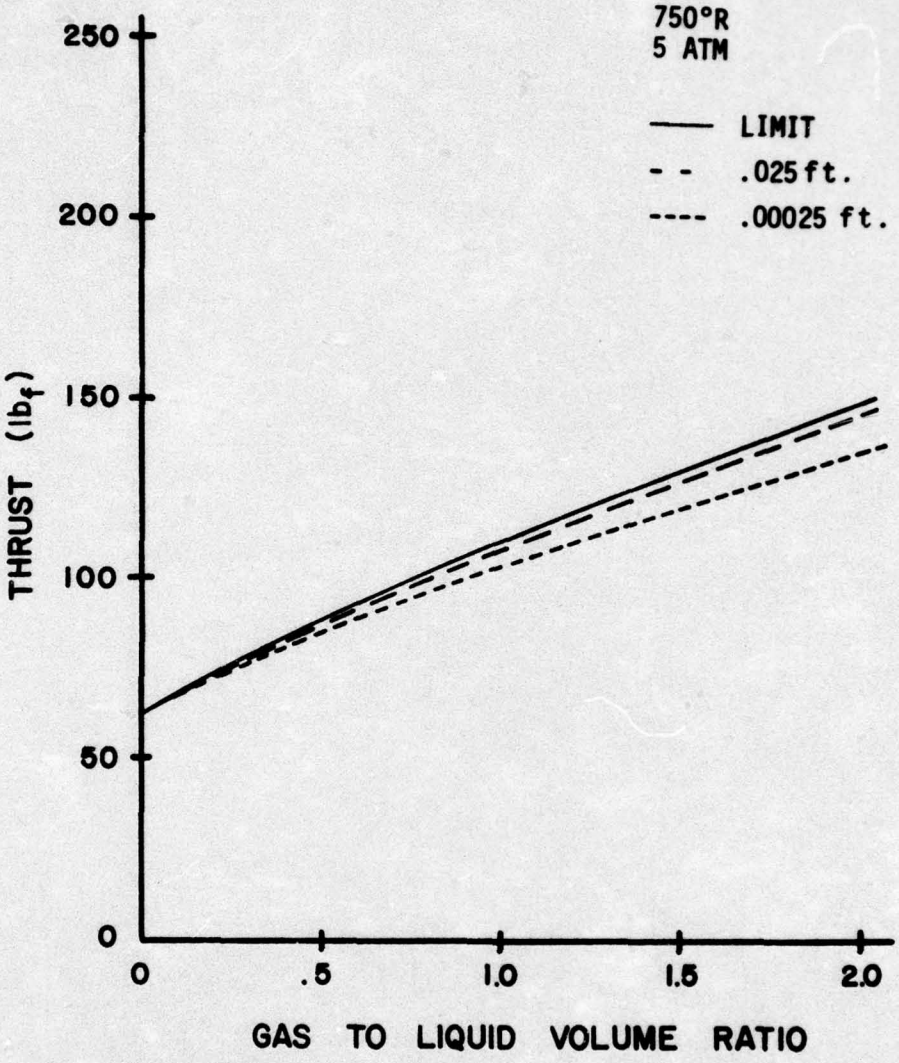

Figure 1.1 Effect of Bubble Size on Thrust

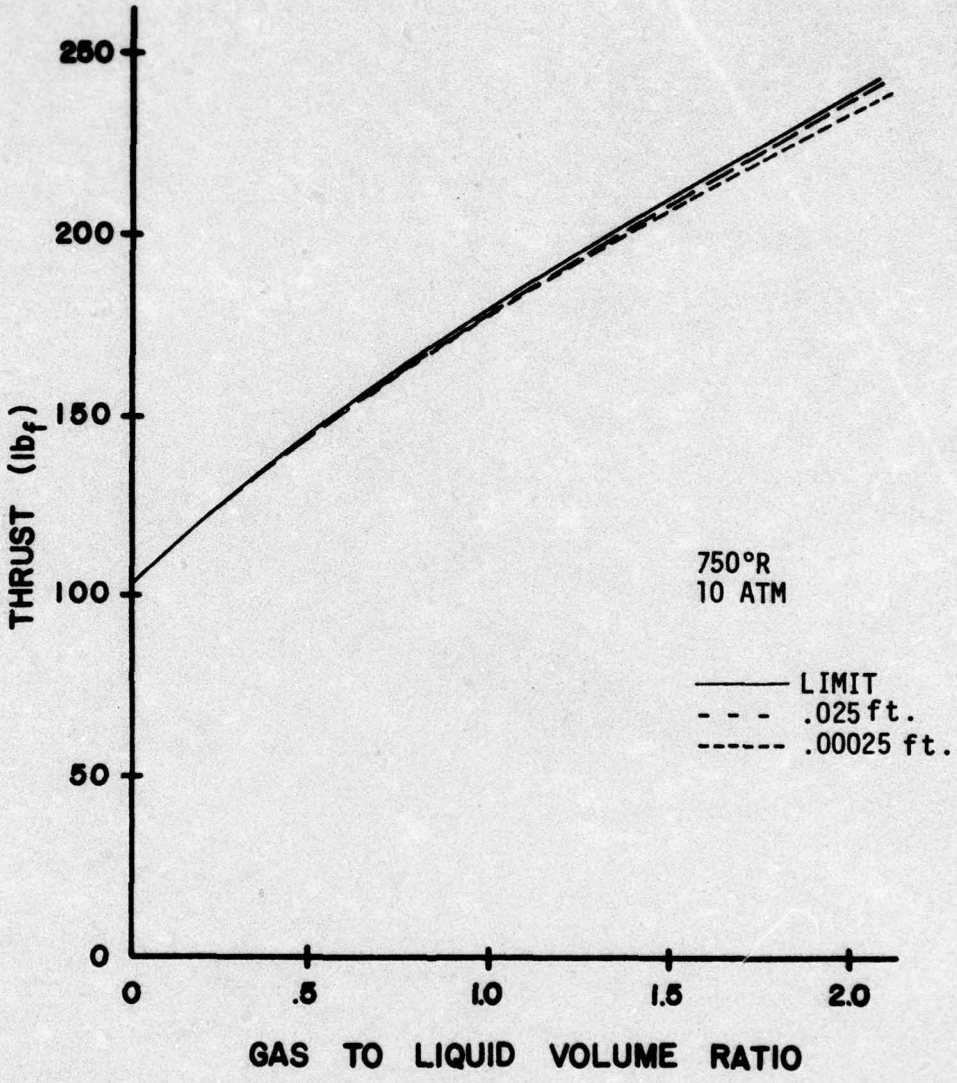

Figure 1.2 Effect of Bubble Size on Thrust

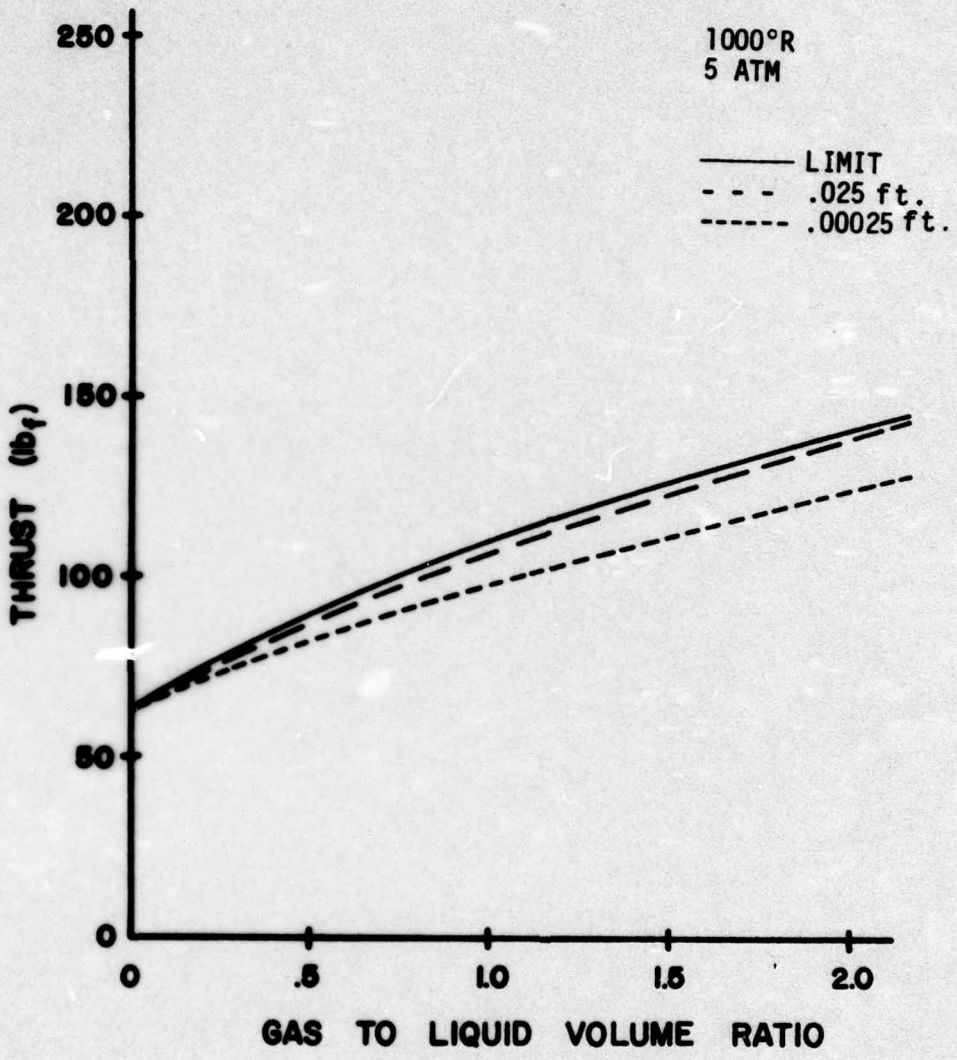

Figure 1.3 Effect of Bubble Size on Thrust

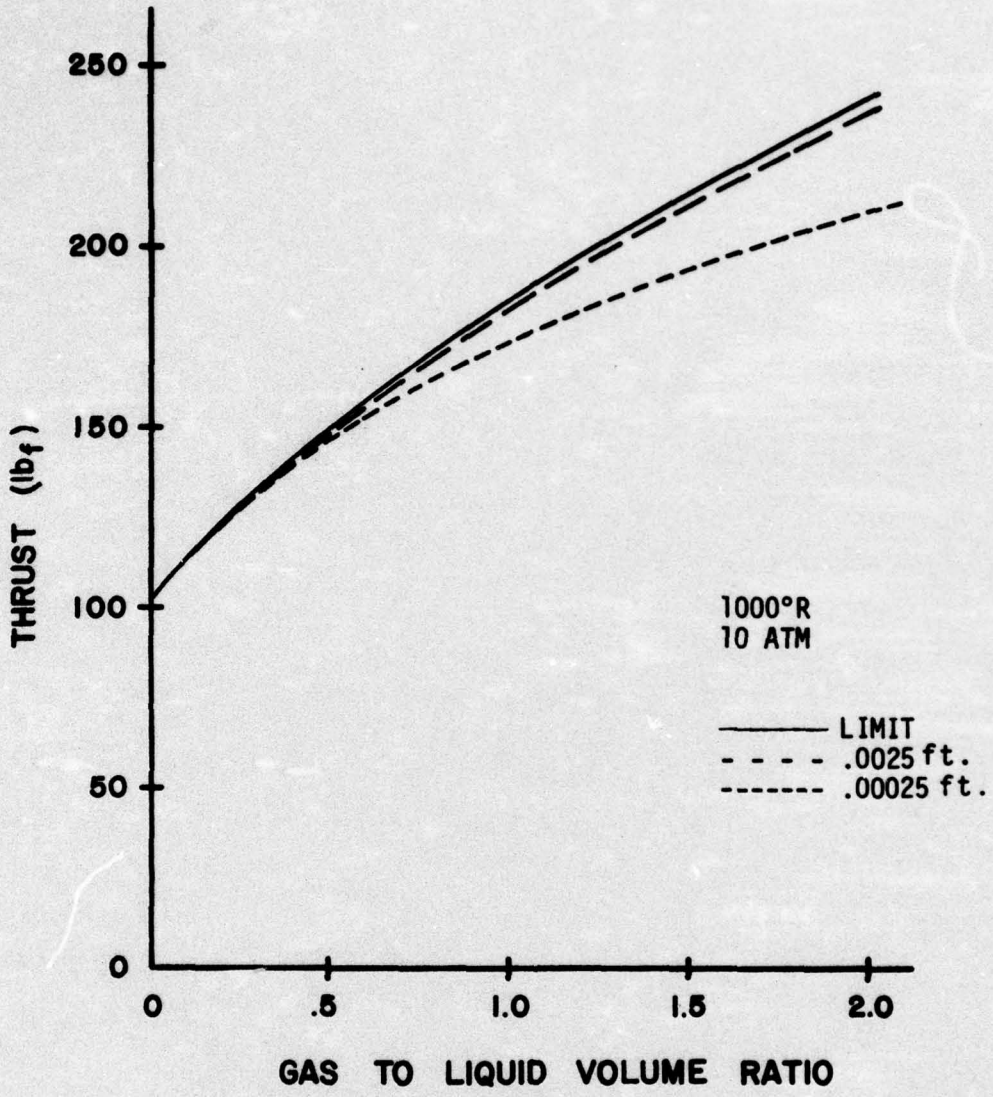

Figure 1.4 Effect of Bubble Size on Thrust

TABLE 1.1 THRUST AS A FUNCTION OF GAS INLET CONDITION WITH INLET BUBBLE RADIUS OF .00025 FEET

INLET VOLUME RATIO OF GAS TO LIQUID	THRUST lb_f							
	*P_o = 5 ATM				P_o = 10 ATM			
	NOT ADIABATIC		ADIABATIC		NOT ADIABATIC		ADIABATIC	
	*T_o = 750	T_o = 1000	T_o = 750	T_o = 1000	T_o = 750	T_o = 1000	T_o = 750	T_o = 1000
0	63.60	63.60	63.60	63.60	102.36	102.36	102.36	102.36
1.0	105.126	98.148	107.957	108.034	179.90	166.38	180.36	180.393
1.5	121.282	111.699	125.092	125.171	209.353	190.731	210.226	210.233
2.0	135.683	124.038	140.180	140.249	235.544	212.565	236.808	236.721

* P_o = Inlet gas pressure

T_o = Inlet gas temperature, °R

TABLE 1.2 THRUST AS A FUNCTION OF GAS INLET CONDITIONS WITH INLET BUBBLE RADIUS OF .025 FEET

INLET VOLUME RATIO OF GAS TO LIQUID	THRUST lb_f							
	*P_o = 5 ATM				P_o = 10 ATM			
	NOT ADIABATIC		ADIABATIC		NOT ADIABATIC		ADIABATIC	
	*T_o = 750	T_o = 1000	T_o = 750	T_o = 1000	T_o = 750	T_o = 1000	T_o = 750	T_o = 1000
0	63.60	63.60	63.60	63.60	102.36	102.36	102.36	102.36
1.0	108.850	107.668	110.066	110.141	182.308	181.090	183.605	183.687
1.5	125.971	124.690	127.266	127.354	212.363	210.459	213.755	213.777
2.0	140.961	139.562	142.273	142.352	238.977	237.308	240.491	240.420

* P_o = Inlet gas pressure

T_o = Inlet gas temperature, °R

TABLE 1.3 MASS RATIO AS A FUNCTION OF INLET CONDITIONS

INLET VOLUME RATIO OF GAS TO LIQUID	MASS RATIO (lbm gas to lbm liquid)			
	*P_o = 5 ATM		P_o = ATM	
	*T_o = 750°R	T_o = 1000°R	T_o = 750°R	T_o = 1000°R
0	0	0	0	0
1.0	.004206	.003155	.008412	.006309
1.5	.006309	.004732	.012619	.009464
2,0	.008412	.006309	.016825	.012619

* P_o = Inlet pressure

* T_o = Inlet temperature

TABLE 1.4 NET INCREASE IN THRUST DUE TO THERMAL ENERGY IN THE GAS

NET THRUST INCREASE (lb_f)		
Inlet Bubble Radius (ft)	Ratio of Gas to Liquid by Mass = .006309	Ratio of Gas to Liquid by Mass = .012619
.000250	2.756 (2.2%)	3.212 (1.5%)
.0250	13.591 (9.7%)	24.945 (10.4%)

of the injected gas does produce increased thrust. The actual percentage increase is contained in parenthesis beside the magnitude of the thrust increase.

CONCLUSION

The proposition outlined in the beginning of this report is shown to be theoretically feasible. The analytical results indicate that the performance of a gas-augmented waterjet can be significantly increased by injecting large radii gas bubbles with a high thermal energy. Furthermore this increase approaches the theoretical limit established in the adiabatic case.

The practicality of this approach must be studied in an actual model. The construction of such a model must be made so that a comparison between actual and theoretical results may be measured. Two systems for achieving large radii bubbles are considered.

The first system considered uses two nozzles and a mechanical valving system to achieve the desired flow. The system would intermittently feed volumes of air and water into opposite nozzles. A schematic drawing is shown in Figure 1.5.

The valves would be connected mechanically or electrically so that when water is fed into one nozzle air is fed into the other nozzle. The flow ratios would be achieved by throttling the gas flow to the desired condition. The advantages of such a system would be to avoid any "water hammer" effect upstream in the water flow. This system would also achieve slug flow directly.

The second system, shown in Figure 1.6, uses only one nozzle. A large plenum chamber located upstream of the nozzle is used to blow bubbles into a relatively slow moving water stream so that the bubbles do not break into smaller bubbles. The air stream is "pulsed" by an electronically controlled valve in order to provide alternate slugs of air and water flow. This system is mechanically simpler than the previous system; however, problems with obtaining homogenous flow due to gravity effects must be overcome.

This study shows tremendous benefit in thrust augmentation can be achieved by capturing the thermal energy in the injected gas and effectively using it to produce thrust. Practical problems in achieving this performance are obvious. The authors feel that experimental work should be performed to study methods of gas injection which will allow these practical problems to be overcome.

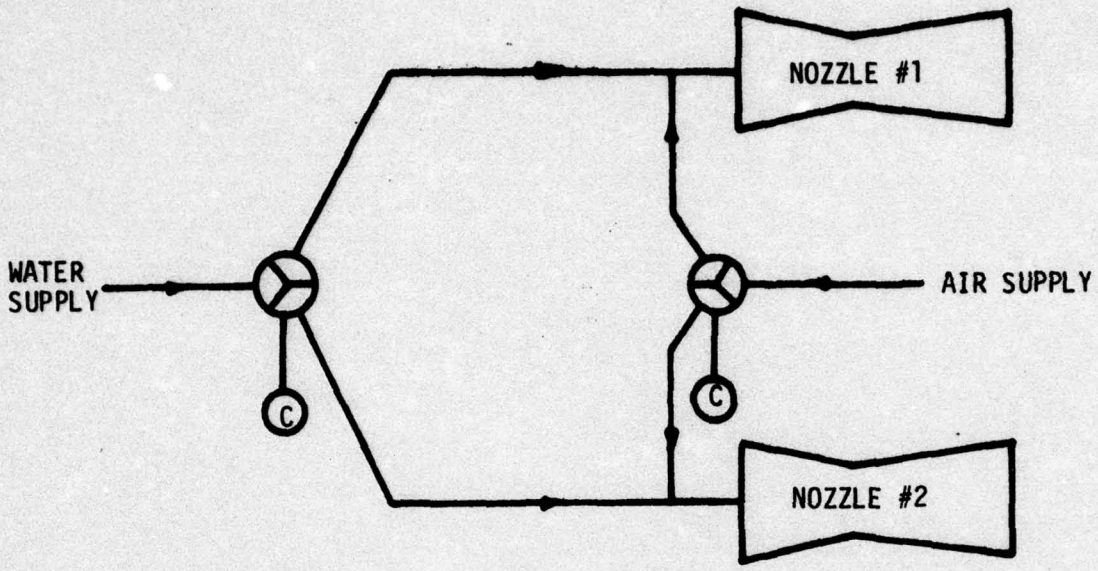

Figure 1.5 Schematic Diagram of Two Nozzle System

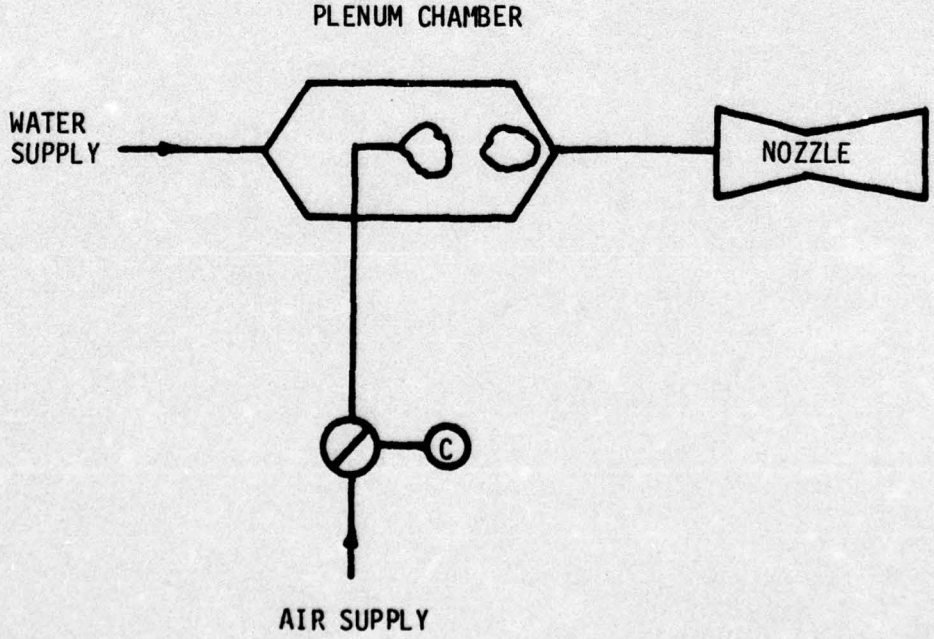

Figure 1.6 Schematic Diagram of Pulse Operation System

PART 2: EXPERIMENTAL INVESTIGATION OF AIR-AUGMENTED WATERJET THRUST NOZZLES

INTRODUCTION

To accomplish the objective of obtaining experimental data on a large scale waterjet, the apparatus shown schematically in Figure 2.1 was designed and constructed. A photographic view of part of this equipment is shown in Figure 2.2.

GENERAL DESCRIPTION OF APPARATUS

The arrangement of components within the experimental facility and their operation are briefly described. Detailed descriptions of major components of the system are given in the next section. (Component numbering is defined in Figure 2.1).

Water Loop

Water is pumped from a 4,000 gallon, open tank (21) through the water intake line (13) by a pump-motor set (10, 11). The water is discharged into a transfer line (25) and the water flow rate is controlled by a manual valve (15). The outlet flow is passed through a venturi flow nozzle (12) for the determination of the water flow rate and then into the air-water mixing chamber (19). The air-water mixture is expelled through the nozzle (18) for the production of thrust. The discharge water from the nozzle is returned to the tank by a flow deflector (20).

Air Loop

For pressures in the mixing chamber of less than 300 psi, the cut-off valve (6) is opened and the manual regulating valve (3) is closed. Air is allowed to flow from a 350 gallon low pressure tank (5) through a low pressure line (27). The air flow rate is measured with a turbine meter (16) and is controlled by a manual flow regulating valve (24) after which it is discharged into the mixing chamber (19). For operation at higher pressures, the cut-off valve (6) is closed and the manual flow regulating valve (24) is opened. Air is discharged from high pressure cylinders (1) into a manifold (2). The air leaves the manifold by a transfer line (26) and the air flow rate is controlled manually by a valve (3).

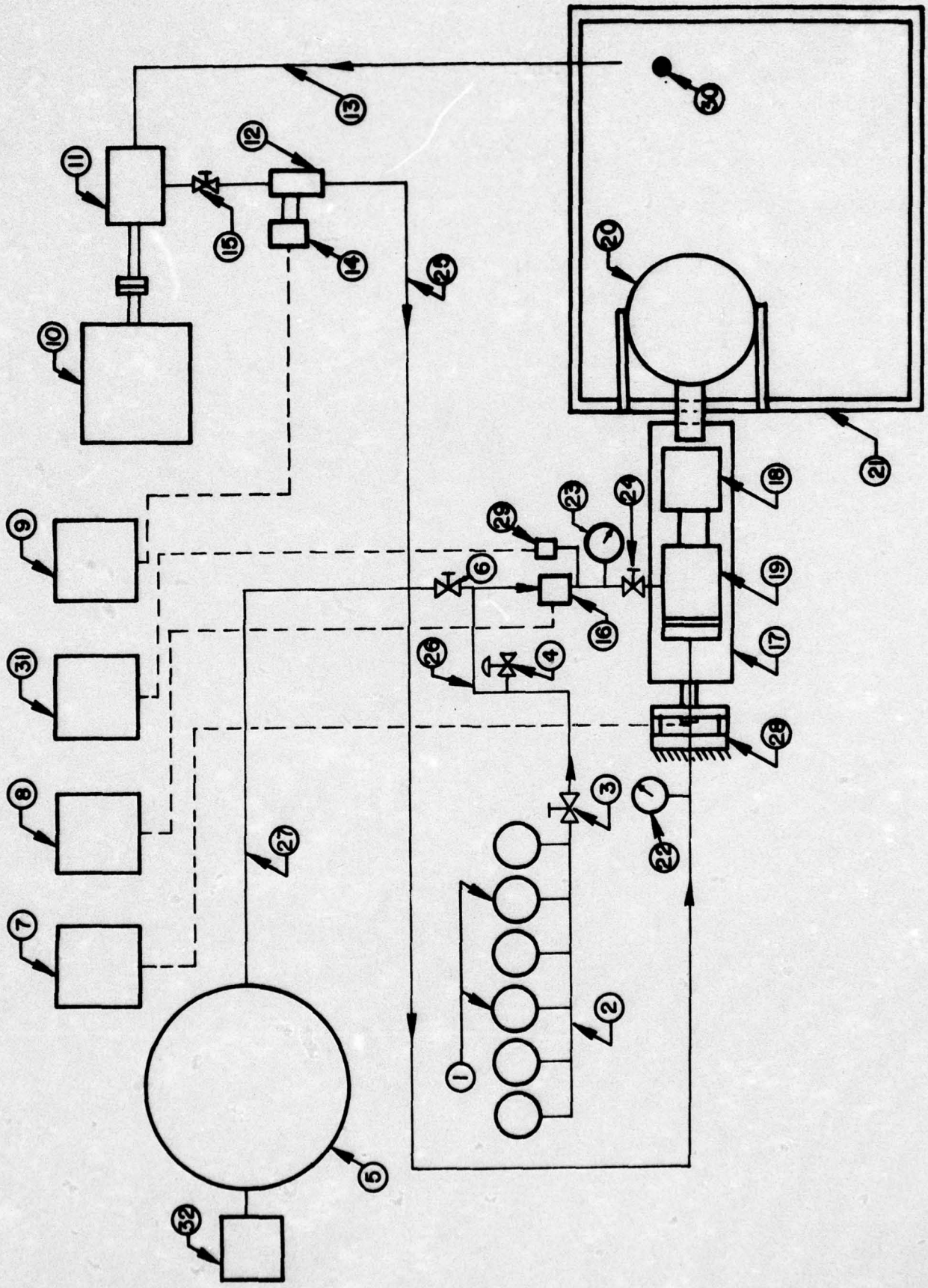

Figure 2.1 Schematic of Gas-Augmented Waterjet Test Facility

EXPLANATION OF NUMBERS ON FIGURE 2.1

1. HIGH PRESSURE AIR CYLINDERS
2. HIGH PRESSURE MANIFOLD
3. MANUAL FLOW REGULATING VALVE
4. PRESSURE RELIEF VALVE
5. LOW PRESSURE AIR TANK
6. CUT-OFF VALVE
7. STRAIN INDICATOR
8. FLOW TOTALIZER
9. INDICATOR, ΔP
10. MOTOR
11. PUMP
12. VENTURI FLOW NOZZLE
13. SUCTION WATER LINE
14. DIFFERENTIAL PRESSURE TRANSDUCER
15. MANUAL FLOW REGULATING VALVE
16. TURBINE METER
17. NOZZLE STAND
18. NOZZLE
19. MIXING CHAMBER
20. FLOW DEFLECTOR
21. OPEN POND
22. PRESSURE GAGE
23. PRESSURE GAGE
24. MANUAL FLOW REGULATING VALVE
25. WATER LINE
26. HIGH PRESSURE AIR TRANSFER LINE
27. LOW PRESSURE AIR LINE
28. THRUST TRANSDUCER
29. THERMOCOUPLE
30. THERMOMETER
31. POTENTIOMETER
32. AIR COMPRESSOR

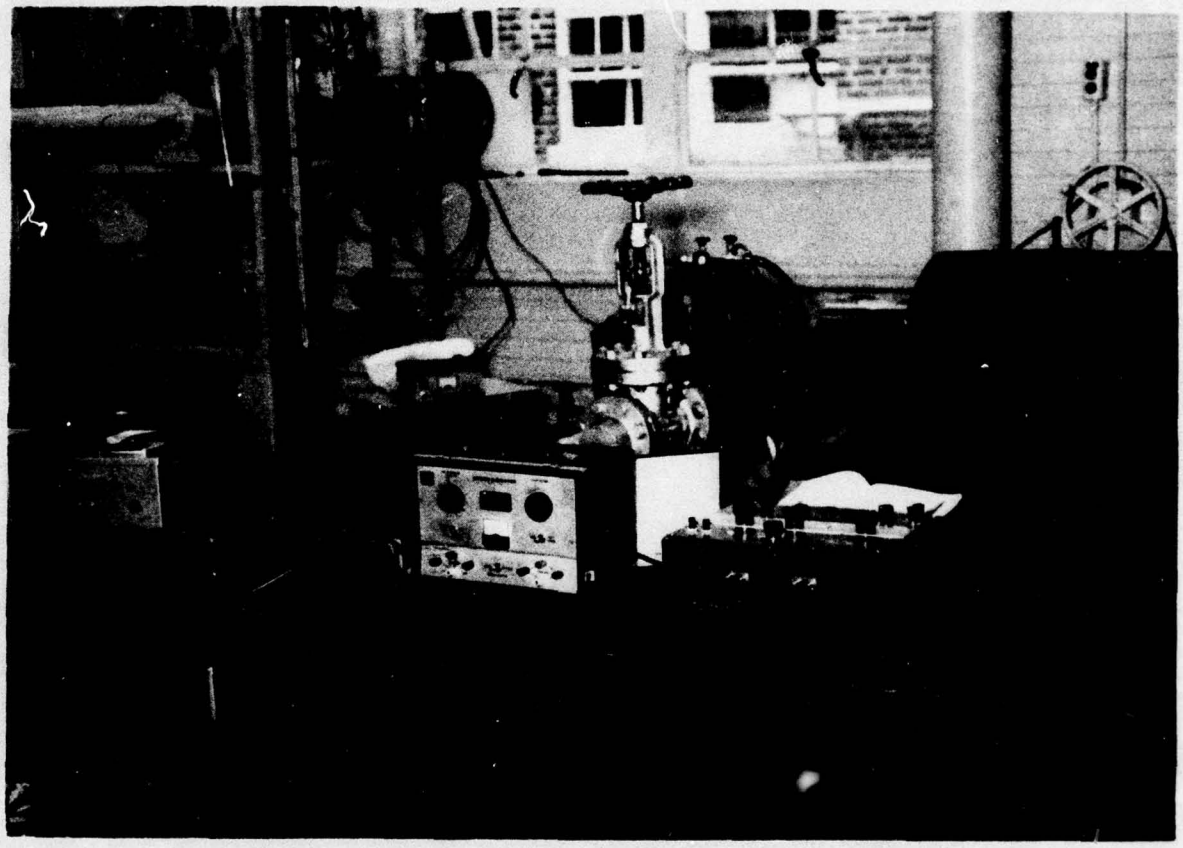

Figure 2.2 Photograph of Pump and Measuring Equipment

Thrust Measurement

The nozzle stand is mounted on two plates. A bar attached to the stand is mounted such that it is forced against the center of a transducer. The transducer consists of a beam clamped at one end and simple supported at the other end. A strain gage is mounted on the back side of the transducer. The thrust produced by the nozzle is transmitted to the thrust transducer (28) which produces strain in the strain gage. The strain is measured by a conventional strain indicator (7). By calibration the strain can be directly related to the pounds of thrust produced.

Temperature Measurement

The open pond water temperature is measured with a thermometer (30). The temperature of the air is measured with a thermocouple (29) which transmits a millivolt signal to the potentiometer (31).

Flow Measurements

The pressure drop in the venturi meter (12) is fed into a differential pressure transducer (14) which has a milliamp output proportional to the pressure drop. The milliamp output is determined by the ΔP indicator (9). By calibration the milliamp output can be directly related to water flow rate.

The air flow rate is measured by a turbine meter (16) which is connected to a totalizer (8) which counts the number of revolutions of the turbine. By calibration, the turbine revolutions can be directly related to the air flow rate.

DETAILED DESCRIPTION OF APPARATUS

The preceding section presented a general description of the test equipment. Several important elements of the system will be described in detail in this section.

Mixing Chambers

A cross-sectional view of the mixing chamber and thrust nozzle is shown in Figure 2.3 and photographs are shown in Figures 2.4 and 2.5. Two types of mixing chambers were used in this work: one had 78, 1/16 inch diameter holes drilled around the circumference of a pipe for air injection

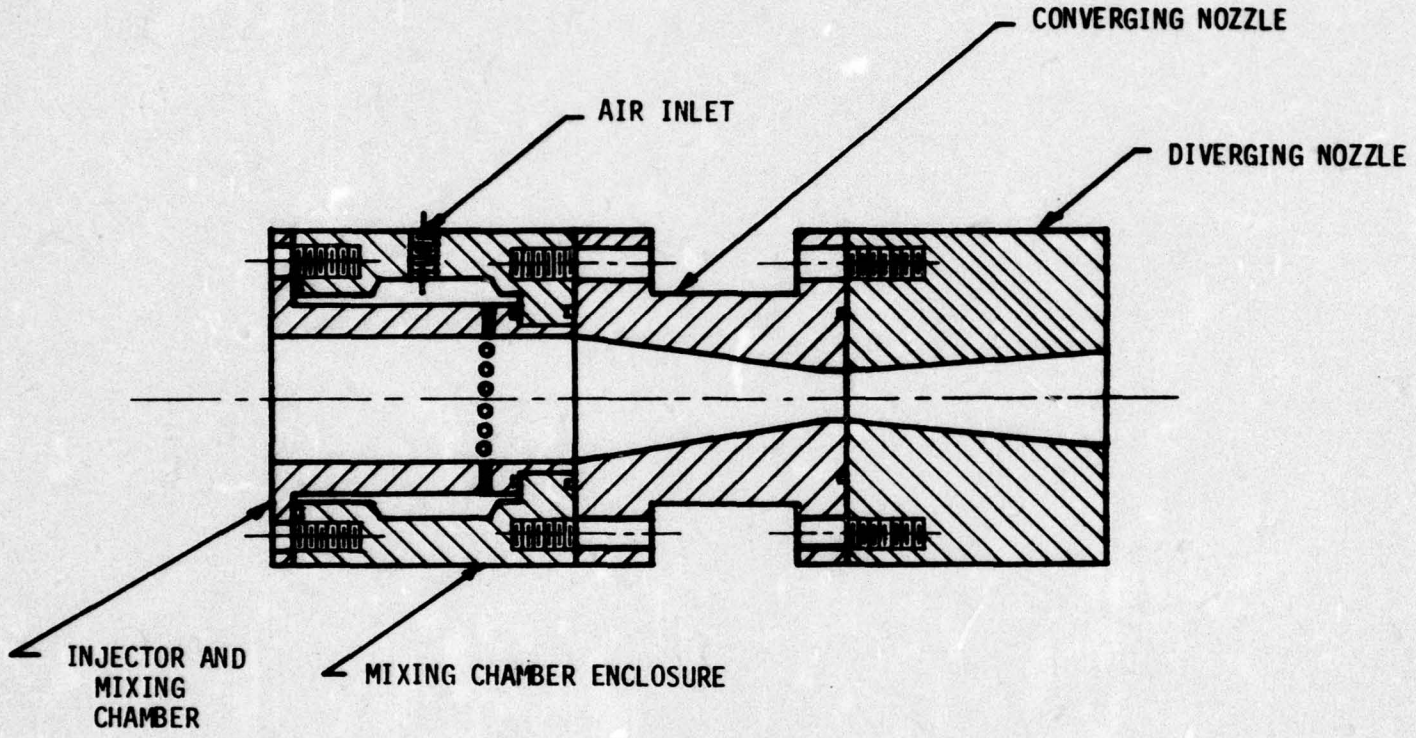

Figure 2.3 Cross-Sectional View of Mixing Chamber and Thrust Nozzle

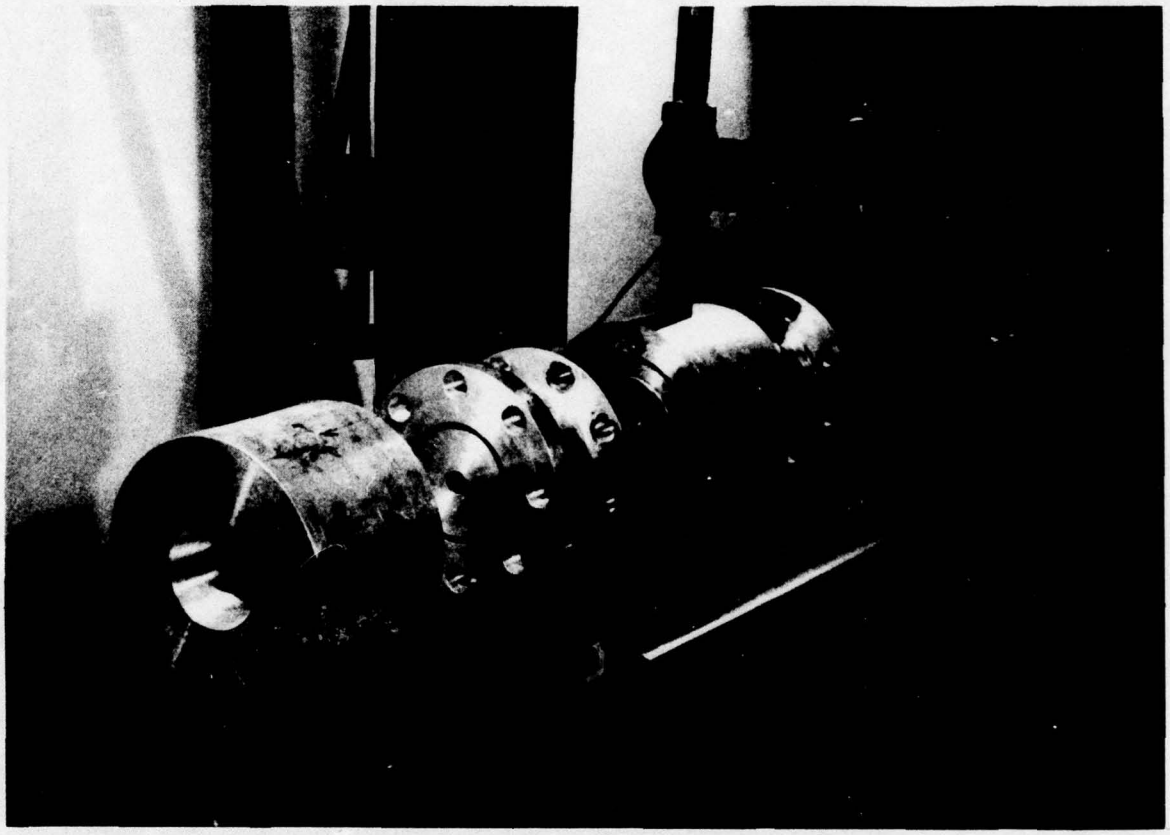

Figure 2.4 Photograph of Components of Mixing Chamber and Thrust Nozzle

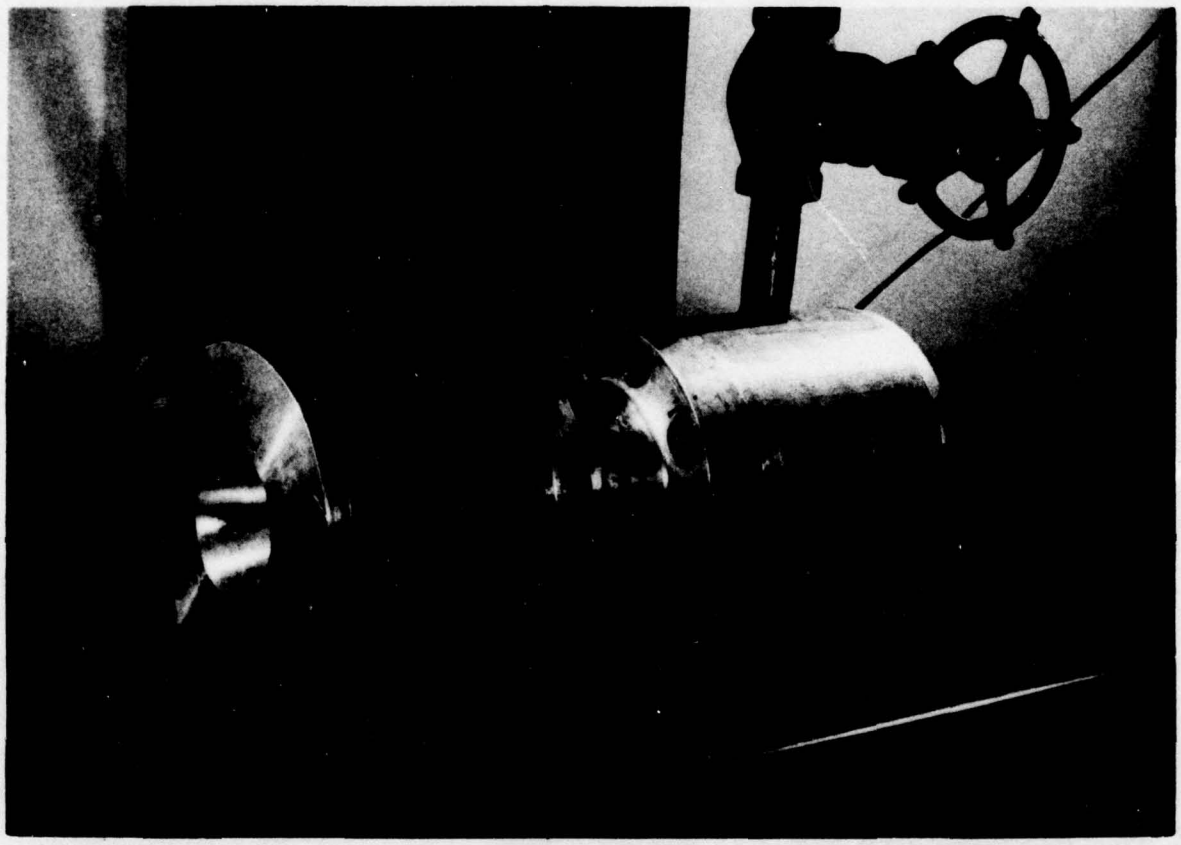

Figure 2.5 Photograph of Mixing Chamber, Thrust Nozzle Assembly

(see Figures 2.6 and 2.7) and the other had 9, 1/4 inch diameter tubes across the flow area of the pipe from which air is injected through 660, 1/32 inch holes (see Figures 2.8 and 2.9). These mixing chambers are subsequently described as "open port" and "cross tube", respectively. The mixing chamber shown in Figure 2.3 is of the open port type.

Two different throat diameters (0.75 inch and 1.25 inch) were used. In addition for each of these throat diameters, three different diffuser angles (5°, 9-1/2° and 15°) were tested.

Nozzle Stand

An elevation view of the nozzle stand is shown in Figure 2.10. The nozzle stand is attached to a concrete floor by a steel plate. Two flexures plates, attached to this plate, support another plate on which the nozzle is attached. A rod attached to the nozzle stand is fixed such that it presses against the thrust transducer (see Figure 2.10). The thrust transducer is rigidly fixed by a steel support attached to the concrete floor. The test stand is equipped with a cable attached to a load platform which allows the nozzle stand to be subjected to a known load for calibration.

Other Equipment

The remaining important equipment was purchased from commercial vendors. Identification and description of this equipment is given in Table 2.1. Detailed description of valves, thermocouples, and transfer lines are not given.

CALIBRATION OF INSTRUMENTS

Venturi Meter

In order to calibrate the venturi meter, it is necessary to have a primary method to determine the water flow rate. This method consists of measuring the volume change of water removed from the open pond in a measured time increment. A depth gage is placed in the pond and a deflector is used to prevent the water

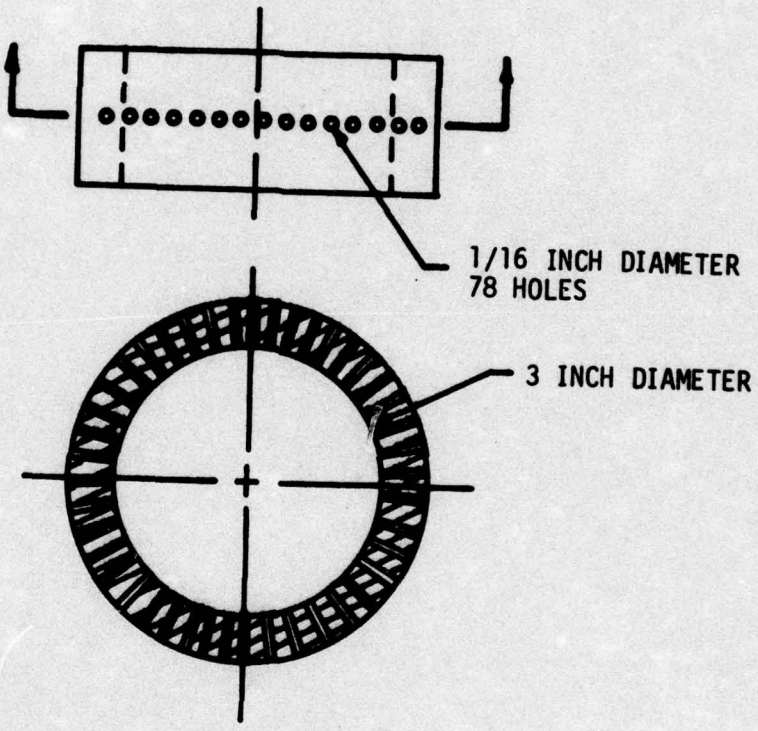

Figure 2.6 Details of Open Port Injector

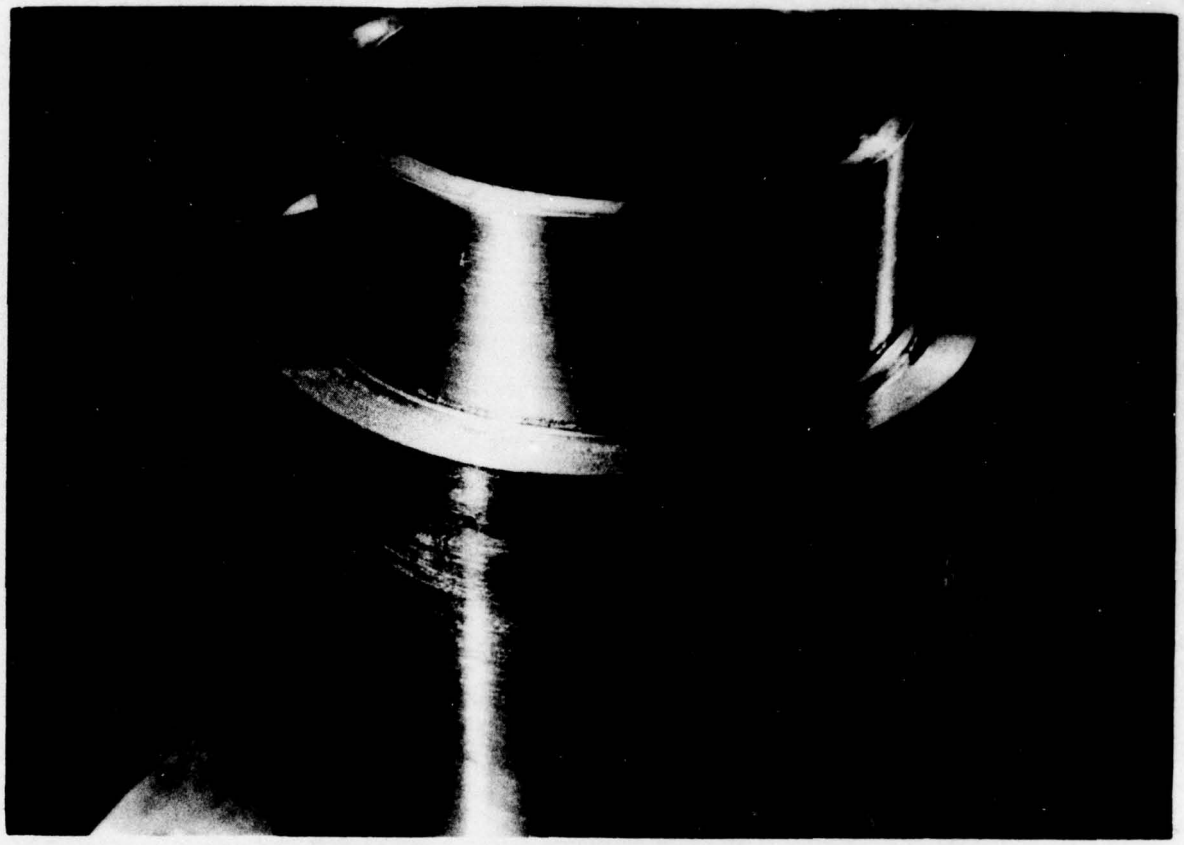

Figure 2.7 Photograph of Open Port Injector

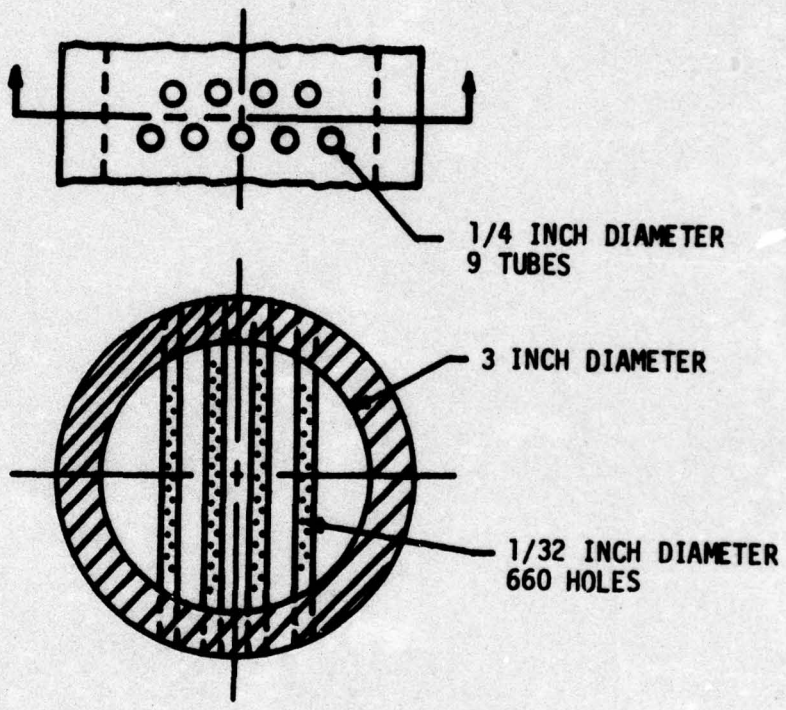

Figure 2.8 Details of Cross Tube Injector

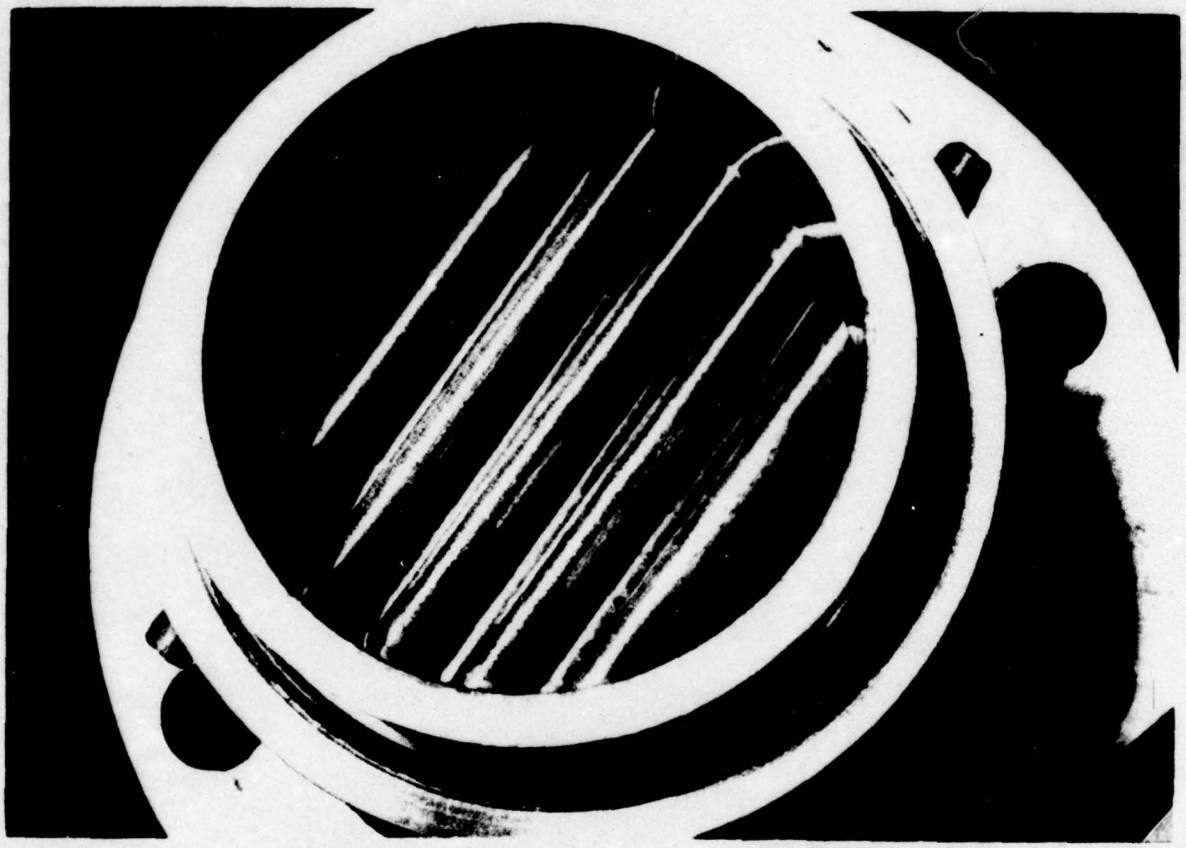

Figure 2.9 Photograph of Cross Tube Injector

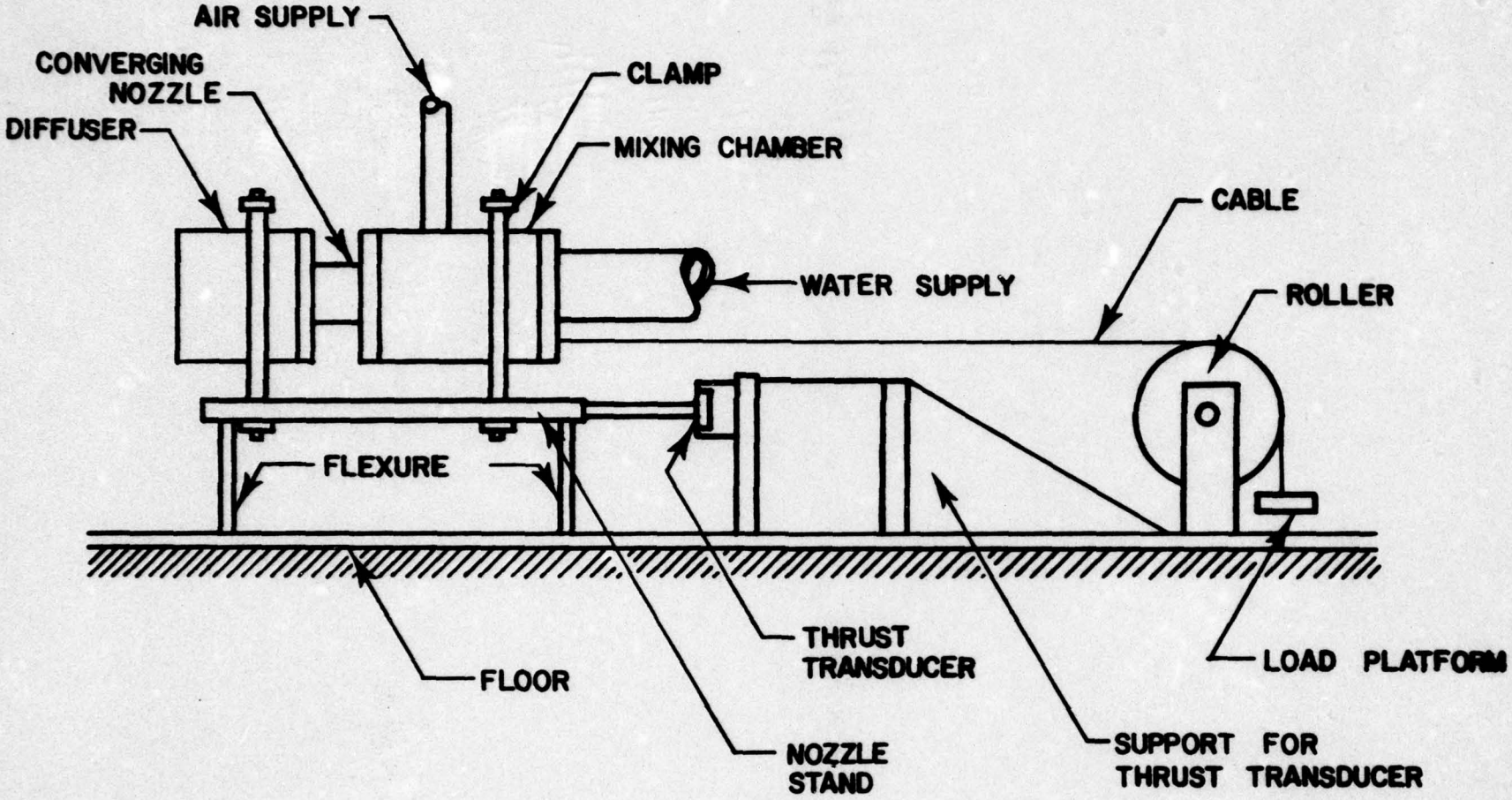

Figure 2.10 Schematic of Thrust Nozzle Test Stand Assembly

TABLE 2.1 DESCRIPTION OF ITEMS USED IN EXPERIMENTAL PROGRAM

ITEM NO. (SEE FIGURE 2.1)	DESCRIPTION OF ITEM	MANUFACTURER
7	SR-4 Strain Indicator	Baldwin-Lima - Hamilton Corporation
8	Totalizer for Turbine Meter	ITT Barton
9	Simpson Model 373 Meter	Simpson Electronic Co.
10	125 Horsepower Electric Motor	Reliance, Inc.
11	Model 3316, Two Stage Centrifugal Pump	Goulds Pumps, Inc.
14	1151 DP Pressure Transmitter	Rosemont
16	1-1/4 inch Turbine Meter	ITT Barton
31	Millivolt Potentiometer - Model 8686	Leeds and Northrup Co.

from returning to the pond. By measuring the change in depth of the pond in a measured time increment, the water flow rate can be calculated by computing the mass of water removed (= volume of water removed multiplied by water density) and dividing this mass by the time increment. Thus, the milliamp output of the ΔP indicator can be directly referenced to the mass flow rate. The venturi meter was calibrated by this method over the range of water flow rates encountered in the experimental tests.

Turbine Meter

The turbine meter totalizer is factory calibrated with a specified accuracy of $\pm$ 1/4% of actual flow. The totalizer reads directly in gallons which is easily converted to mass by multiplying by the air density. Of course, the flow rate is the amount of mass divided by the time increment.

Strain Indicator

The strain indicator reads the number of micro inches of strain. A cable and platform on which weights could be used to load the thrust transducer was devised (see Figure 2.10). By placing weights of known magnitude on the load platform, a calibration of strain versus weight was obtained. Of course during the calibration no air or water was allowed to flow. The amount of strain with zero air or water flow and zero weight on the platform (i.e., the "zero reading") varied with temperature due to thermal expansion. Consequently at the beginning of each run, it was necessary to obtain the zero reading. It was determined, however, that the differential strain produced by a given load is independent of the zero reading to within 1%. In addition, the thrust versus strain curve was found to be linear within 1%.

Temperature

The thermometer (30) is a secondary standard based on the National Bureau of Standards Specification. The thermocouple (29) output was checked against the boiling point and ice point of water at atmospheric pressure.

TEST PROCEDURE

A brief description of the test procedure is given below. The description is divided into two catagories: preparation activities and testing activities.

Preparation Activities

1. Calibrate all instruments as described in section on calibration.
2. Turn on pump and allow water to flow through loop until thermal equilibrium between water and piping is achieved.
3. Set air flow valves as indicated in the section: "Description of Apparatus".
4. Turn on power to instruments, zero air-flow totalizer and balance potentiometer.
5. Turn off pump after thermal equilibrium is achieved.
6. Approximately 30 seconds after pump is stopped, obtain zero reading of strain indicator.
7. Turn on pump and bleed differential pressure transducer to remove any trapped air.
8. Set the manual water flow regulating valve to achieved the desired water flow rate. The test is ready to begin.

Testing Activities

1. Set the manual air flow regulating valve to give the desired ratio of air to water flow rate. (The amount of air being supplied can be judged from the back pressure produced in the mixing chamber).
2. Begin counting time with a stop watch. Note the number of gallons indicated by the air totalizer when the stop watch is started.
3. Record the following data immediately after beginning the test:
   (1) milliamp output of ΔP indicator (for flow rate of water),
   (2) micro inches of strain (for thrust),

(3) millivolt output of thermocouple measuring air temperature, (4) air supply pressure, (5) pressure in mixing chamber and (6) the temperature of the pond water. A typical data sheet is shown in Figure 2.11.

4. Reset water flow rate to desired magnitude and repeat steps (1) through (3).
5. After making approximately five tests, shut off pump to check whether the zero reading of thrust transducer has shifted. If zero has shifted more than 2% discard data and repeat tests. Begin with item 7 of preparation activities in order to carry out additional tests.

Figure 2.11 Typical Data Sheet

DATE: November 1, 1976

TEST SECTION: #1

THROAT DIAMETER: 1-1/4

DIVERGING HALF ANGLE 15°

AIR INJECTION: CROSS TUBE

RUN NO.	STRAIN	WATER			AIR					COMMENTS
		ΔH (μ_a)	TEMP. (°C)	PRESS. (psig)	NO.	TIME MIN.	TIME SEC.	TEMP. (°F)	PRESS. (psig)	
1	3435	30	24	178	20.5		15	55	198	3090-Strain Meter Zero at Start of Test.
2	3588	36	24	252	27		15	55	270	
3	3718	48	24	300	27		15	39	305	
4	3466	26.5	24	200	30		15	50	212	
5	3443	36	25	170	13		15	52	180	
6	3547	47	25	198	6		15	55	360	3090 at End
7	3316	36	25	156	7		17	48	265	Put in Plate: 2970 at Start of Test
8	3350	36	25	187	13.8		15	52	245	
9	3168	18.5	25	100	9.6		15	52	235	
10	3070	9.5	25	49	6.7		15	55	227	
11	3110	9.5	25	74	19		15	55	205	
12	3040	6.5	26	33	8.7		15	55	195	
13	3060	6.5	26	50	19.1		15	55	175	
14	3162	20.5	26	80	4.7		15	55	175	
15	3190	19.8	26	101	11.4		15	55	165	2990 at End

RESULTS AND CONCLUSIONS

Visual Results

The performance of the nozzle is greatly affected by the amount of air used. Therefore, the optimum design of the injector-nozzle system depends on the amount of air being used. In order to demonstrate this fact, several photographs were taken under varying conditions. Figures 2.12 and 2.13 show the waterjet discharging from the diverging portion of the 15° half-angle nozzle. In Figure 212 the water flow rate is 340 gpm and the air-water ratio is 0.00025. The jet does not "fill" the outlet cross-sectional area. In Figure 2.13 the air-water ratio is .009 with the same water flow rate. The waterjet fills the nozzle exit area in this case. These photographs show dramatically that, in nozzle design, it is necessary to consider the air-water ratio.

The same phenomena is illustrated by Figures 2.14, 2.15, and 2.16 which are photographs of a waterjet discharging from the throat of a converging nozzle. The air-water ratio varies from zero in Figure 2.14 to 0.004 in Figure 2.16.

Experimental Results

Approximately 300 tests were conducted by the procedure outlined previously. These tests covered the range of variables shown in Table 2.2 .

TABLE 2.2 TEST CONDITIONS

Water Flow Rate	100 $\frac{gal}{min}$ to 450 $\frac{gal}{min}$
Inlet Water Pressure	50 psia to 450 psia
Air-Water Ratio (by Mass)	0 to .008
Converging Section, Nozzle Throat Diameter	.75 inch and 1.25 inch
Diverging Section, Half-Angle	5°, 9-1/2°, and 15° cross tube and open port

Results of these tests can be conveniently plotted as the ratio of actual thrust to ideal thrust, $T = T_A/T_i$, versus the air-water ratio on a mass basis, $w \equiv \dot{m}_A/\dot{m}_w$. The ideal thrust, T_i, is computed as follows:

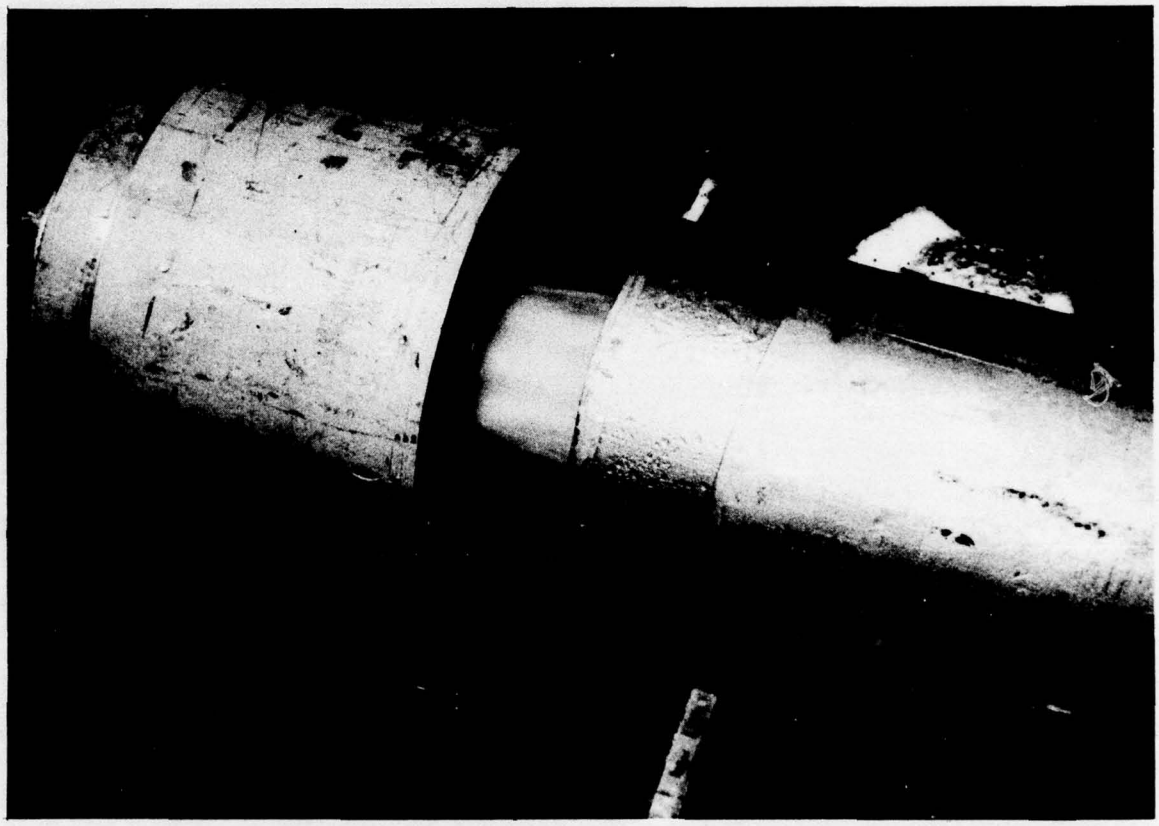

Figure 2.12 Discharge Jet with Low Air-Water Ratio in Diverging Section

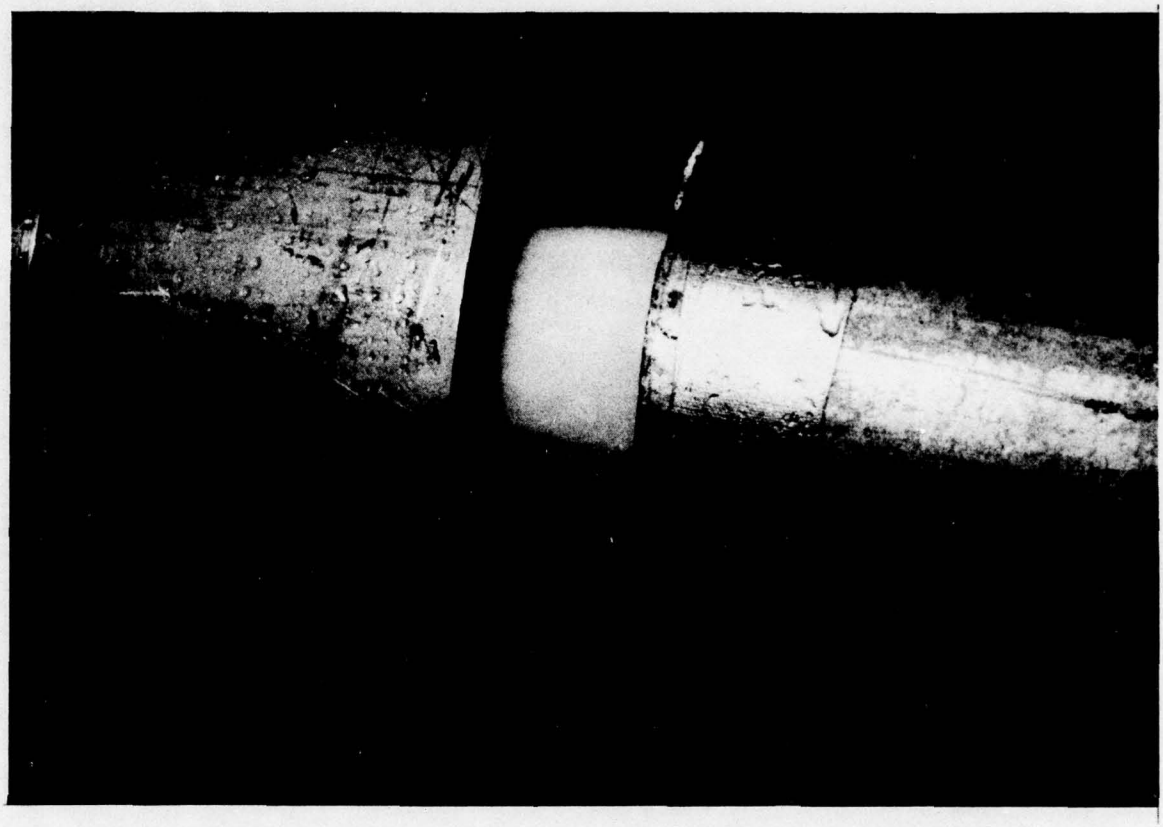

Figure 2.13 Discharge Jet with High Air-Water Ratio in Diverging Section

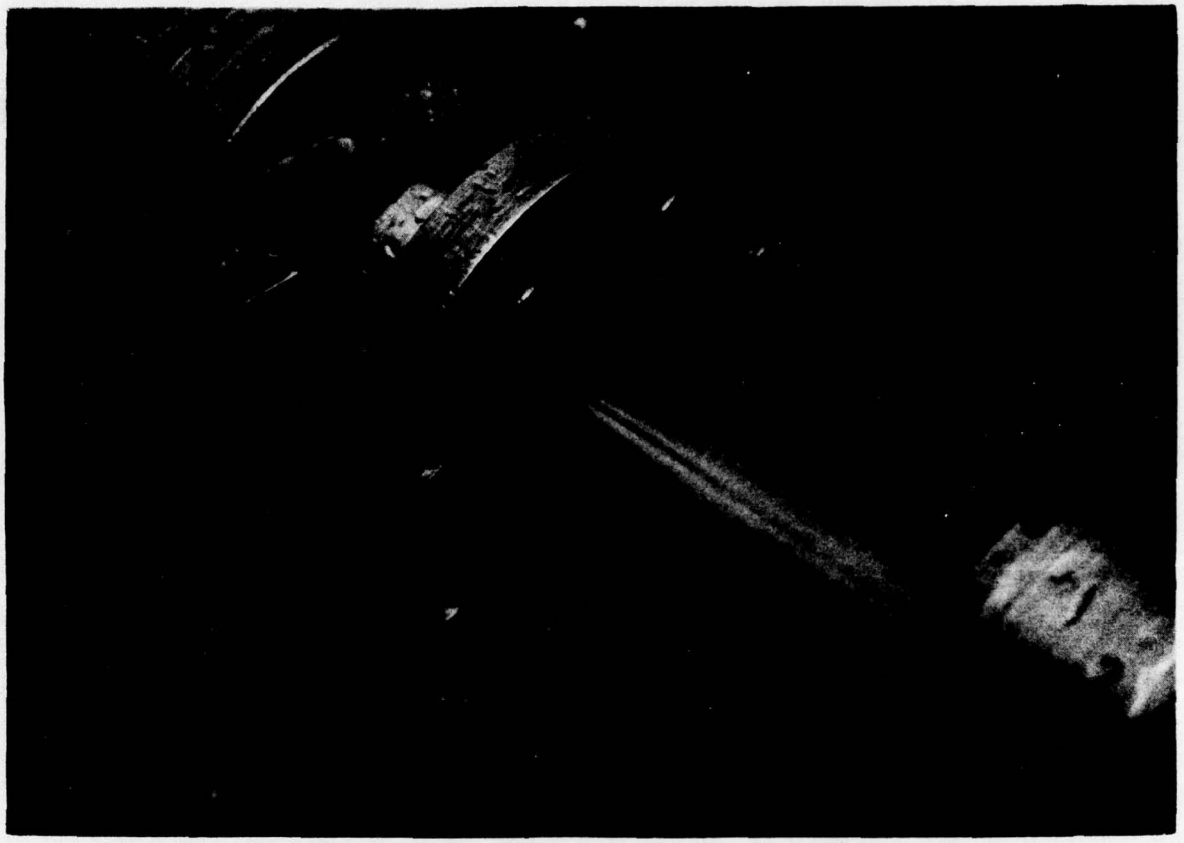

Figure 2.14 Discharge Jet with No Air Injection, Converging Section

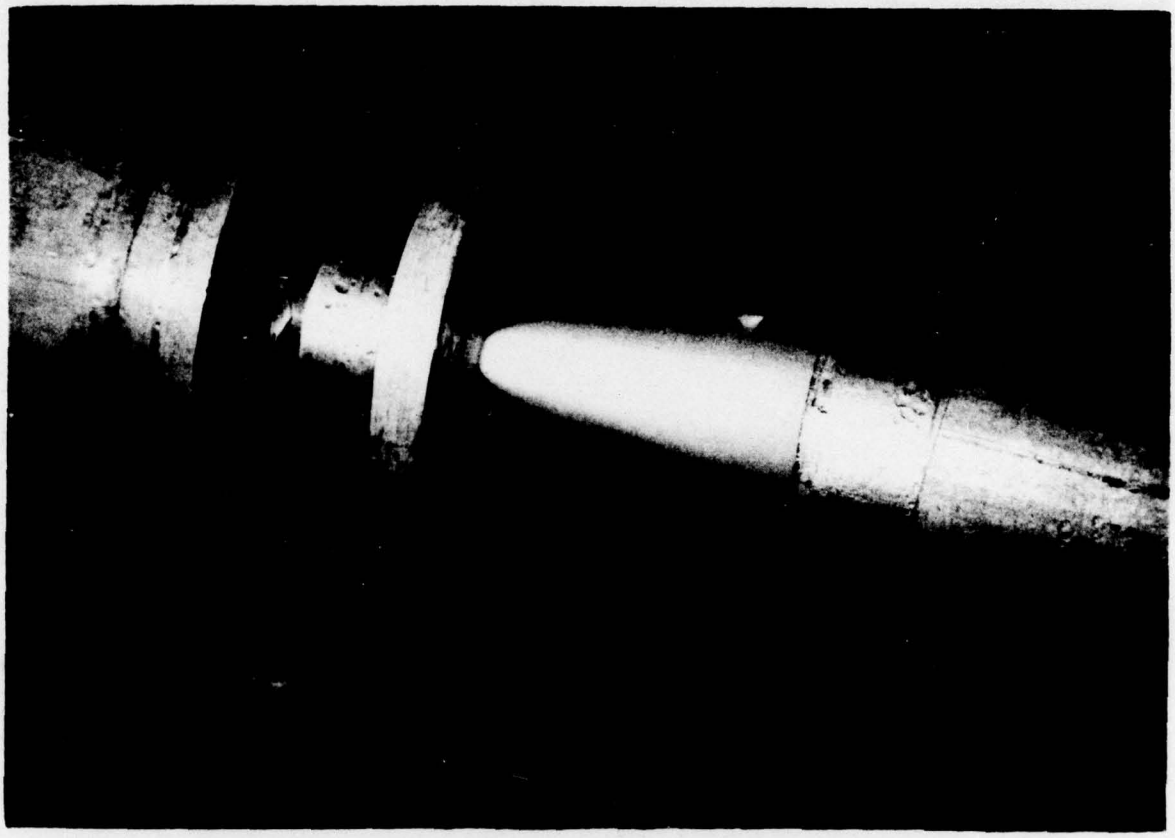

Figure 2.15 Discharge Jet with Low Air-Water Ratio, Converging Section

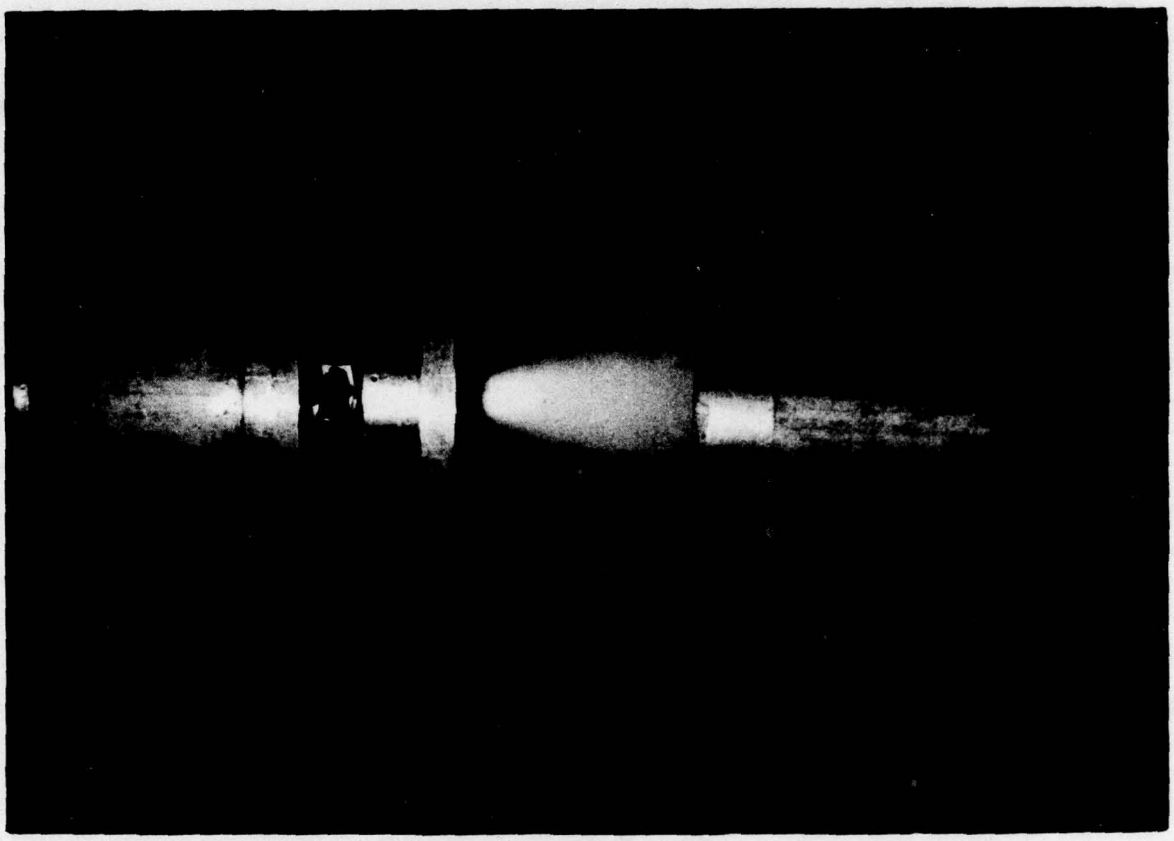

Figure 2.16 Discharge Jet with High Air-Water Ratio, Converging Section

$$T_i = \dot{m}_w V_i$$

where $\dot{m}_w$ is the mass flow rate of water, and

V_i is the exit velocity achieved by the water in an isentropic expansion to atmospheric pressure

Thus, the non-dimensional thrust T will be a relative measure of thrust augmentation achieved by air-injection. It is to be expected that, for a given geometrical configuration, the non-dimensional thrust, T, will increase with air-water ratio, w.

The geometrical configurations tested include twelve different cases obtained by considering all combinations of the following variations:

2 types of injectors (cross tube and open port)
2 nozzle throat sizes (.75 inch throat and 1.25 inch throat)
3 diverging section half-angles (5°, 9-1/2°, and 15°)

Data for dimensionless thrust, T, versus air-water ratio, w, are plotted on the same graph for both type injectors for a given nozzle size and diverging half-angle. Thus, the results are plotted in six graphs shown in Figures 2.17 through 2.22.

Several important trends and conclusions based on these data are noted below:

1. Generally the thrust increases with air-water ratio as expected.
2. Thrust can be increased by 20 percent or more by air augmentation at air-water ratio, w, of 0.003.
3. Cross tube injection produces greater thrust than injection from side ports. This is almost certainly due to better mixing of the air with the water. Increased mixing produces a greater transfer of energy to the water. This conclusion is supported by the fact that open port injection is the least effective for the smaller nozzle throat. This nozzle produced higher pressures for a given flow rate. The higher pressure retards mixing of the air for a given air-water ratio.

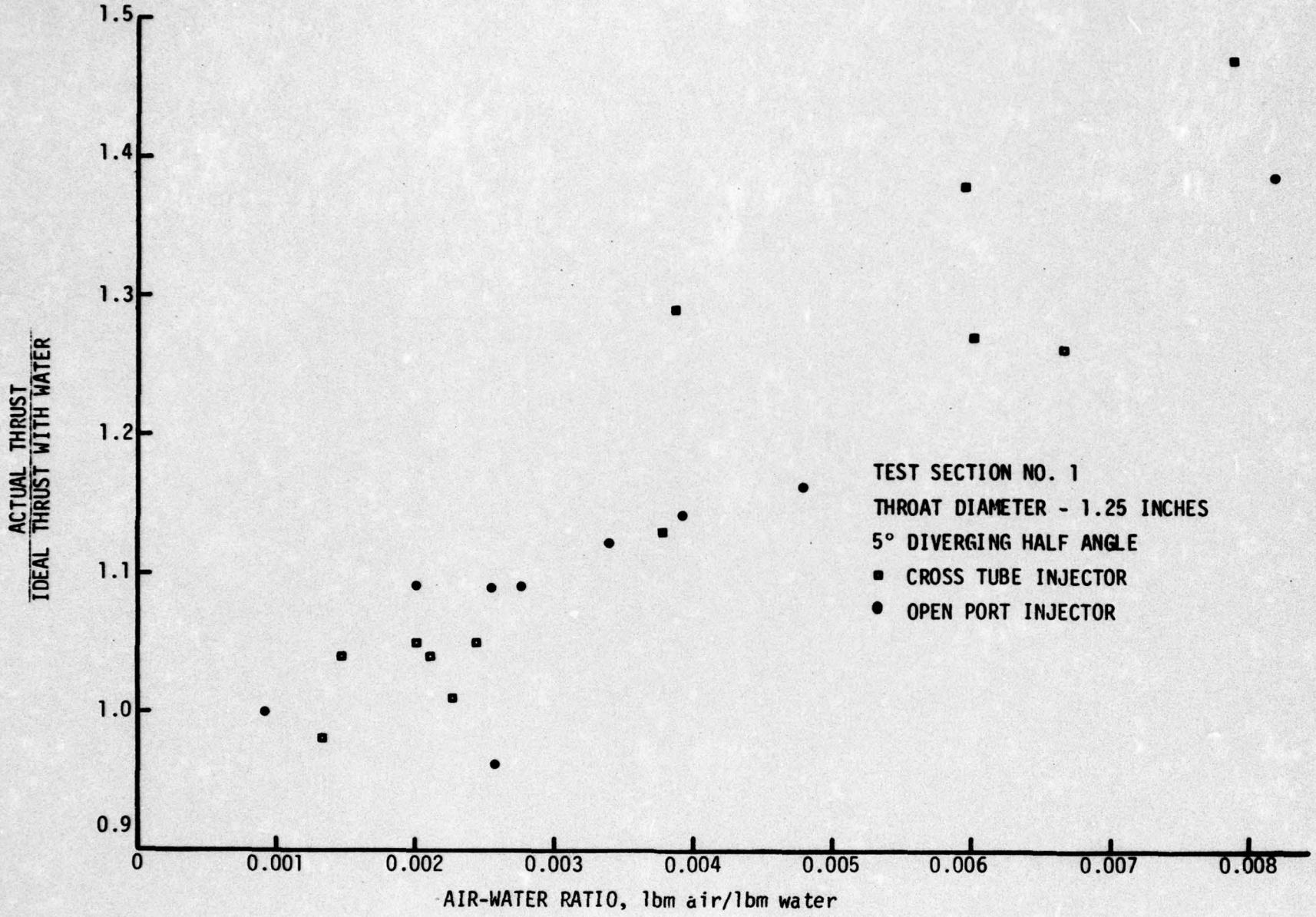

Figure 2.17 Dimensionless Thrust vs. Air-Water Ratio

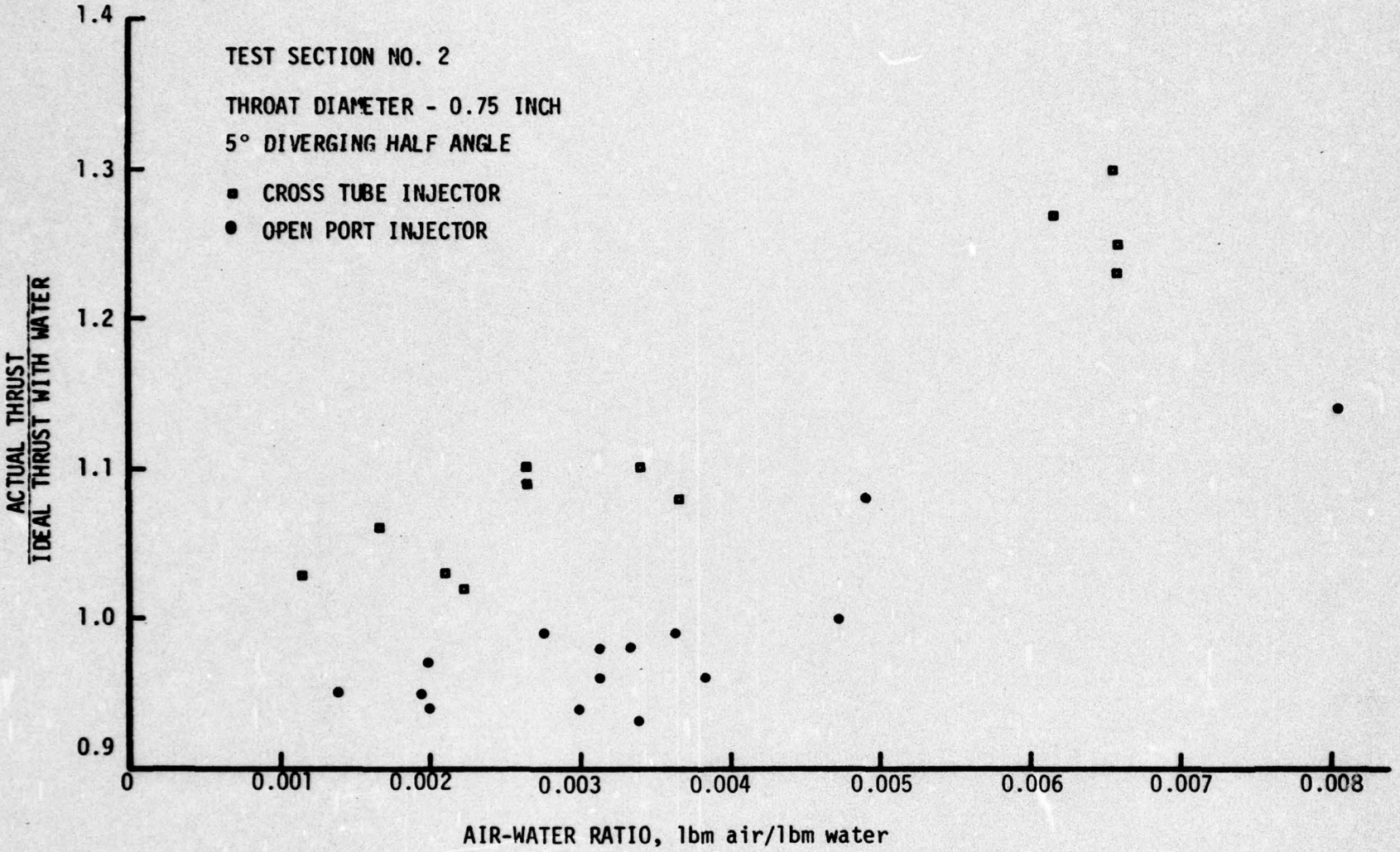

Figure 2.18 Dimensionless Thrust vs. Air Water Ratio

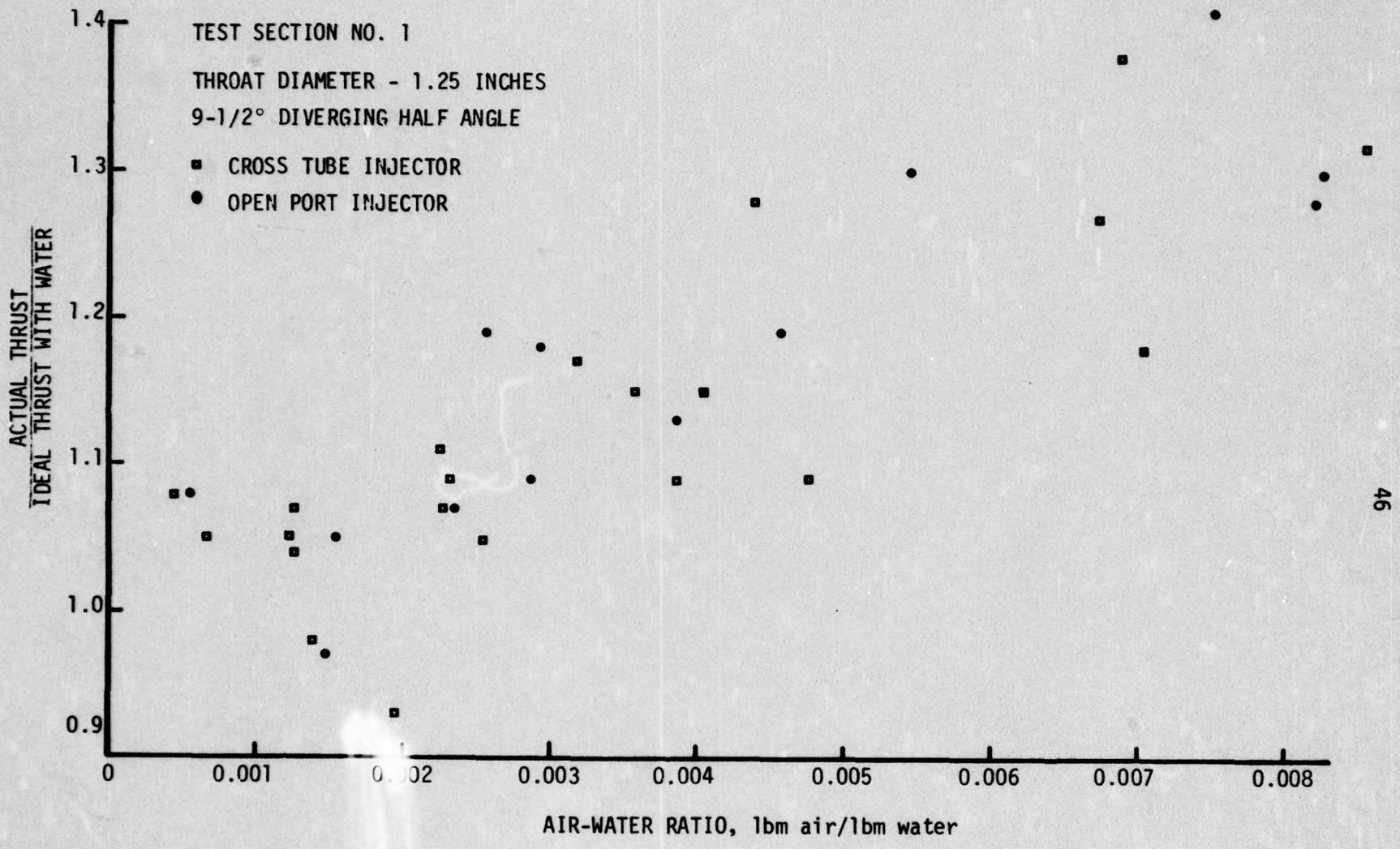

Figure 2.19 Dimensionless Thrust vs. Air-Water Ratio

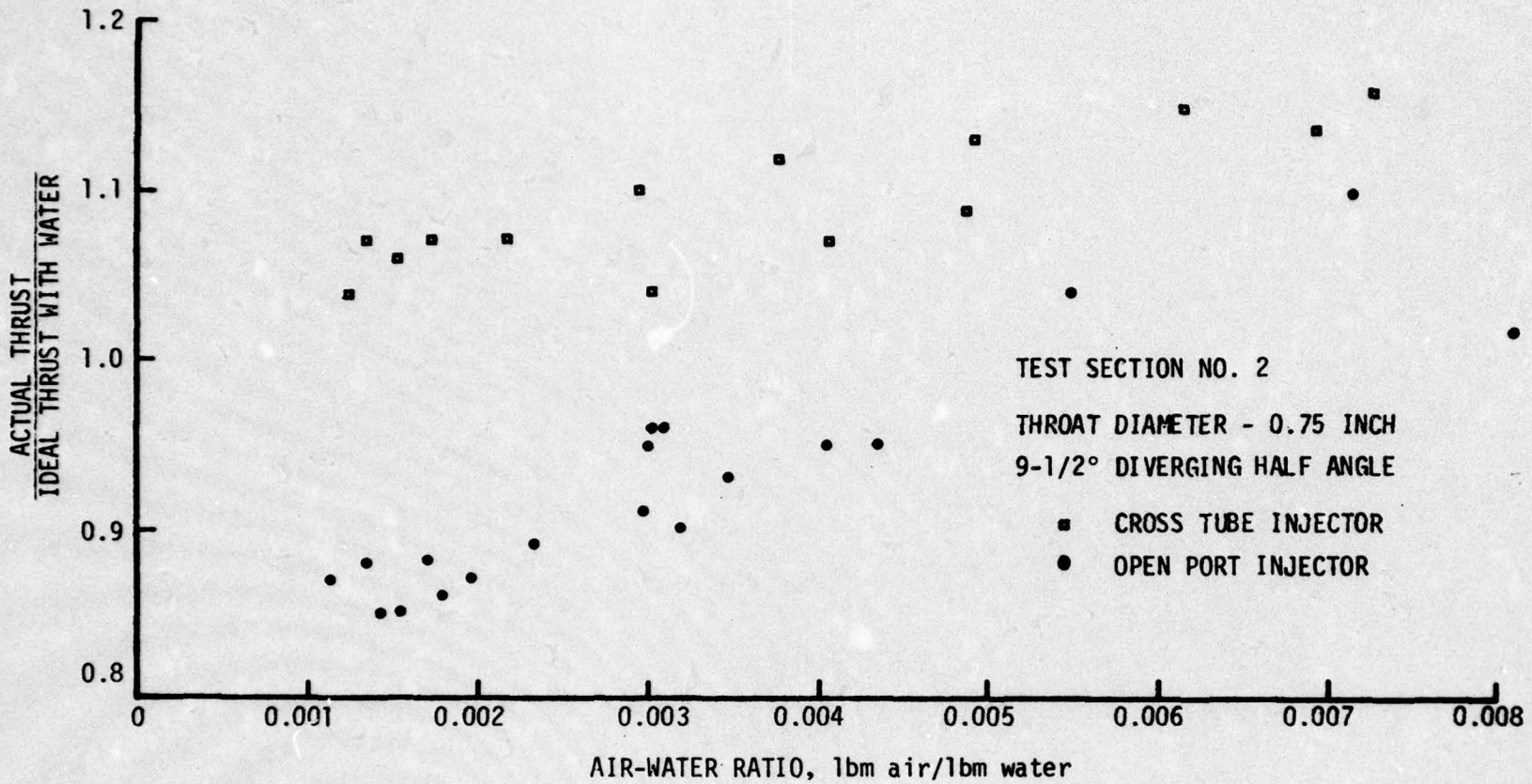

Figure 2.20 Dimensionless Thrust vs. Air-Water Ratio

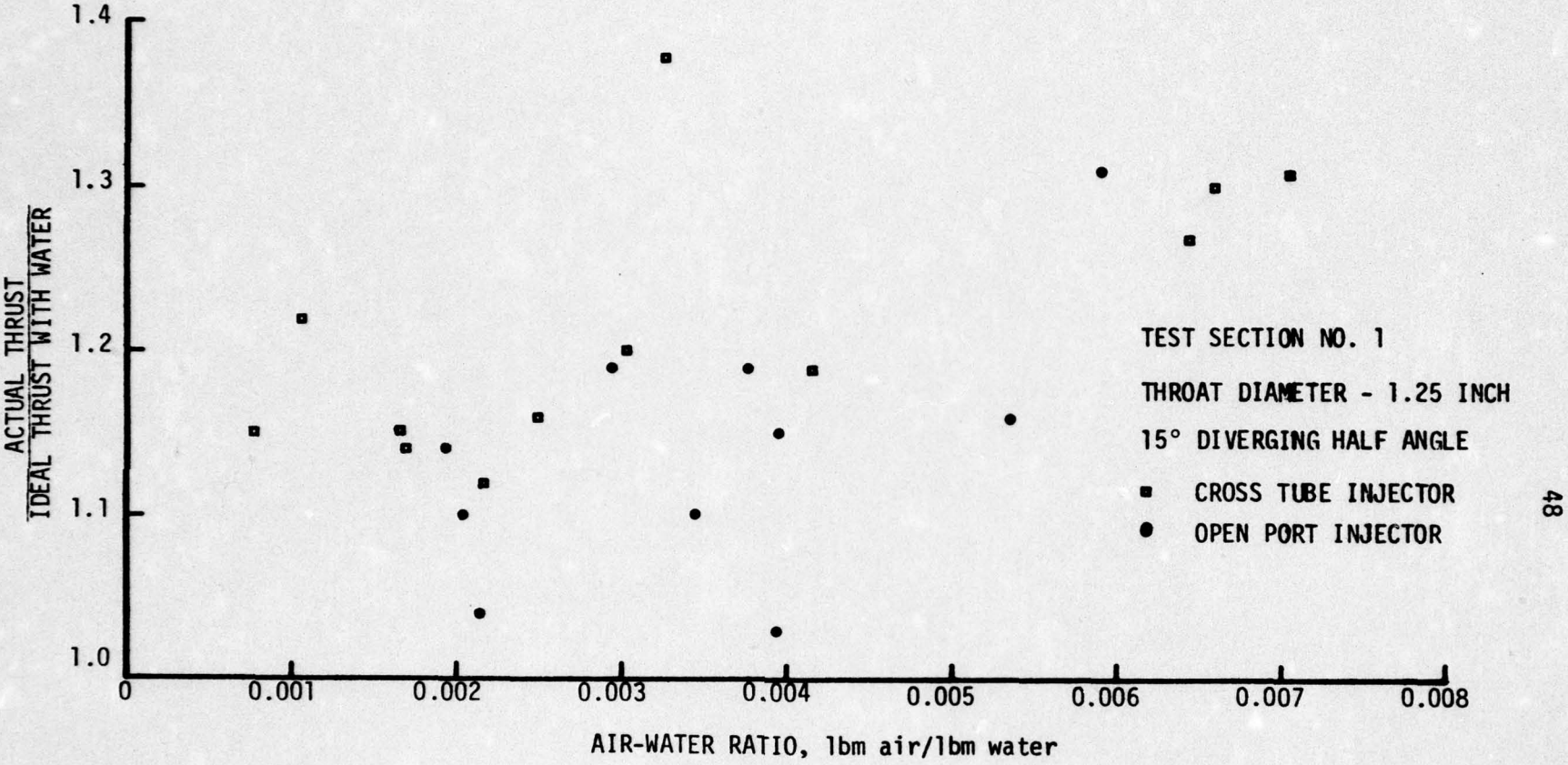

Figure 2.21 Dimensionless Thrust vs. Air-Water Ratio

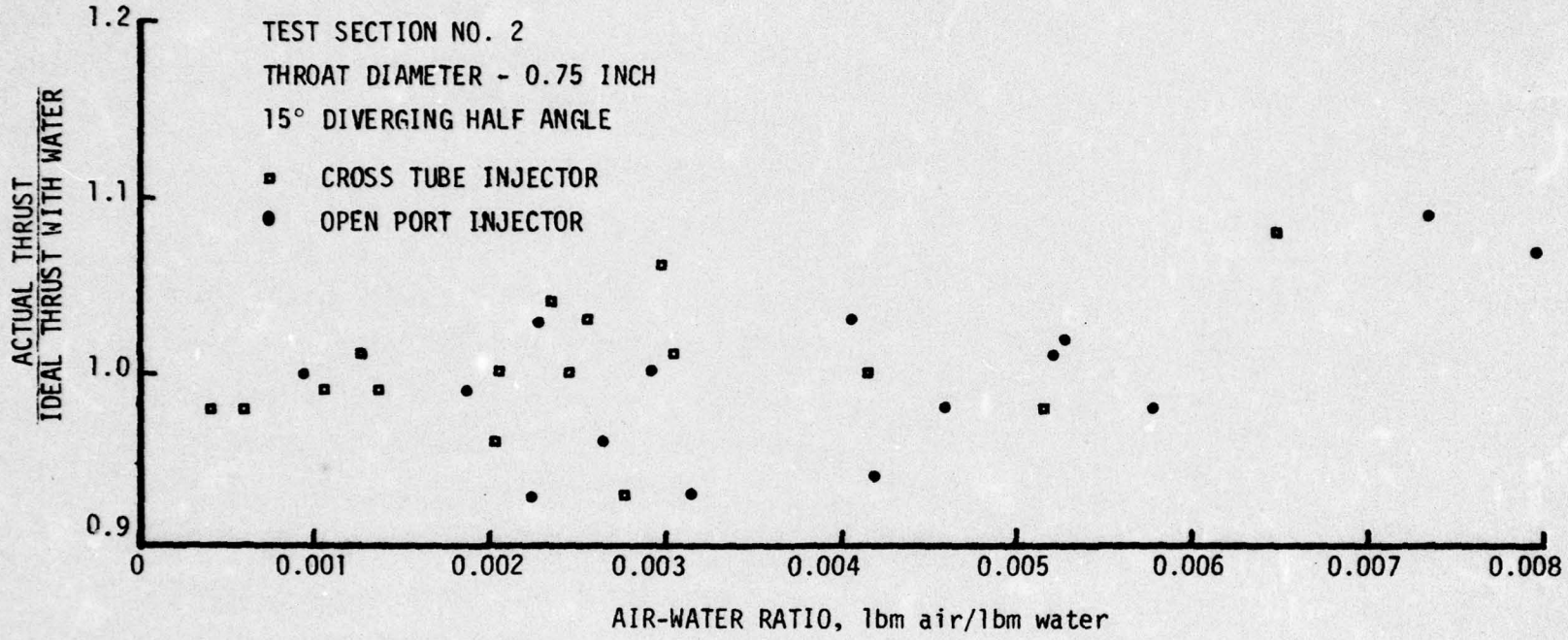

Figure 2.22 Dimensionless Thrust vs. Air-Water Ratio

4. The data from the present work generally agrees with earlier work by the authors [1] for smaller nozzles. In that data thrust augmentation up to 20 percent occurred at an air-water ratio of .004. However, the present data does show an increase in thrust for larger nozzles. Therefore scaling does have some effect.
5. Performance is only slightly affected by the half-angle of the diverging section.
6. Some data, particularly for injection from open ports, indicate a dimensionless thrust less than 1. This presumably occurs because of poor air-water mixing results inefficient expansion. Thus, the actual thrust even with air injection can be less than the ideal thrust for no air injection.
7. In Figures 2.17 through 2.22, the percentage thrust augmentation is indicated by the ratio of actual to ideal thrust. The actual percentage augmentation, measured by actual thrust with air injection divided by actual thrust without air injection, would be greater than the data shown in Figures 2.17 through 2.22. This is true because the ideal thrust (for isentropic expansion) is always greater than the actual thrust (for irreversible expansion) for the same water flow rate and no air injection.

REFERENCES

1. Maxwell, T. T., J. F. Stansell, G. Maples, D. F. Dyer, "Performance of Gas-Augmented Waterjet Propulsion System", Contract No. N00014-72-C-0177, September 1973.

2. Maxwell, T. T., "Thrust of an Air-Augmented Water Jet with a Converging-Diverging Nozzle", Masters Thesis, Auburn University, 1973.

UNCLASSIFIED

SECURITY CLASSIFICATION OF THIS PAGE (When Data Entered)

REPORT DOCUMENTATION PAGE	READ INSTRUCTIONS BEFORE COMPLETING FORM
1. REPORT NUMBER: N00014-75-C-0936	2. GOVT ACCESSION NO. / 3. RECIPIENT'S CATALOG NUMBER
4. TITLE (and Subtitle): PERFORMANCE OF AIR-AUGMENTED WATERJET THRUSTERS.	5. TYPE OF REPORT & PERIOD COVERED: Final Report (4/1/75 - 11/30/76)
	6. PERFORMING ORG. REPORT NUMBER
7. AUTHOR(s): D. F. Dyer, G. Maples, H. T. Cansler and J. C. Maxwell, Jr	8. CONTRACT OR GRANT NUMBER(s): N00014-75-C-0936 NEW
9. PERFORMING ORGANIZATION NAME AND ADDRESS: School of Engineering (ME Department) Auburn University Auburn, Alabama 36830	10. PROGRAM ELEMENT, PROJECT, TASK AREA & WORK UNIT NUMBERS
11. CONTROLLING OFFICE NAME AND ADDRESS: Office of Naval Research	12. REPORT DATE: Nov 30 76
	13. NUMBER OF PAGES: 51
14. MONITORING AGENCY NAME & ADDRESS (if different from Controlling Office): Final rept. 1 Apr 75 – 30 Nov 76	15. SECURITY CLASS. (of this report): Unclassified
	15a. DECLASSIFICATION/DOWNGRADING SCHEDULE
16. DISTRIBUTION STATEMENT (of this Report): Distribution of this document is unlimited. 59p.	
17. DISTRIBUTION STATEMENT (of the abstract entered in Block 20, if different from Report)	
18. SUPPLEMENTARY NOTES	
19. KEY WORDS (Continue on reverse side if necessary and identify by block number): Waterjet Propulsion; Two-Phase Propulsion; Two-Phase Flow; Gas-Augmented Waterjet Propulsion	

20. ABSTRACT (Continue on reverse side if necessary and identify by block number)

This report describes an investigation of the performance of air-augmented waterjet thrusters. The investigation is divided into two parts.

Part 1 describes a study of the injection of large diameter air bubbles to reduce heat transfer between the air and water and, thus, increase the thrust. This study is done analytically by solving the appropriate, governing equations. The results indicate that the approach is very worthwhile since thrust can be increased ten percent as compared to air-

DD FORM 1 JAN 73 1473 EDITION OF 1 NOV 65 IS OBSOLETE S/N 0102-014-6601

UNCLASSIFIED

SECURITY CLASSIFICATION OF THIS PAGE (When Data Entered)

046870 4B

20.

augmentation with small bubbles. Several practical systems are discussed for injecting large air bubbles.

Part 2 is an experimental investigation of the thrust produced under a wide range of conditions. The results show that a thrust increase of more than 20% can be achieved by air-augmentation. Further, the performance improves for larger thrust nozzles.